Please cite this article in press as: Hong et al., Metal-organic frameworks for fast electrochemical energy storage: Mechanisms and opportunities, Chem (2023), https://doi.org/10.1016/j.chempr.2023.02.016

Chem

CellPress

Review

Metal-organic frameworks for fast electrochemical energy storage: Mechanisms and opportunities

Chulgi Nathan Hong,[1] Audrey B. Crom,[2] Jeremy I. Feldblyum,[2,*] and Maria R. Lukatskaya[1,*]

SUMMARY

Metal-organic frameworks (MOFs) have the potential to rival or even surpass traditional energy storage materials. However, realizing the full potential of MOFs for energy storage with competitive performance at industrially relevant scales requires a unified approach from electrochemists and synthetic and material chemists. This review aims to bridge the knowledge gap between electrochemists and scientists working in the field of MOFs. We introduce the basic concepts of energy storage devices, including charge storage mechanisms, and highlight the interconnected nature of the material, electrode, and cell parameters that can significantly affect the metrics of energy storage devices. The design principles of MOFs are then discussed in relation to the parameters that must be considered for their use in fast electrochemical energy storage devices. Finally, we discuss the characterization techniques necessary to unveil the charge storage mechanism in MOF-containing energy storage devices, as this understanding is critical to drive their rational design.

INTRODUCTION

Energy storage devices having high energy density, high power capability, and resilience are needed to meet the needs of the fast-growing energy sector.[1] Current energy storage devices rely on inorganic materials[2] synthesized at high temperatures[2] and from elements that are challenged by toxicity (e.g., Pb) and/or projected shortages of stable supply (e.g., Li and Co).[3] In this context, systems that do not rely on Li as the charge carrier ion, such as those based on Na, and that utilize organic-based materials as electrodes provide a conceptually attractive alternative.[4,5] These systems can be made fully from abundant elements such as Na, C, N, and O and can be potentially produced by sustainable methods.[4–6] Practical implementation of systems that possess such compositions remains challenging for several reasons: (1) transition to lithium-free energy systems requires the design of materials that are capable *of reversibly accommodating larger* cations,[5–7] (2) insufficient *chemical*[8] and *electrochemical stability*[5] of organic-based materials leads to unsatisfactory cycle life,[6,9] and (3) an additional set of requirements is imposed on material properties and electrode and device architectures for fast electrochemical energy storage (EES) applications (e.g., high power).[10] In addition to a high density of redox-active sites (and hence, high capacities), these sites should be readily accessible to both ions and electrons to achieve fast-charging kinetics.[5,11] Hence, the material should have sufficient electronic conductivity and ion accessibility (Figure 1).[2,9]

Recently, metal-organic frameworks (MOFs) have emerged as a distinct class of materials for EES.[13] MOFs are constructed via coordination bonding between nodes (metal ions or ionic metal clusters) and ligands (organic molecules) that results in

THE BIGGER PICTURE

Electrochemical energy storage (EES) devices are typically based on inorganic materials made at high temperatures and often of scarce or toxic elements. Organic-based materials represent attractive alternatives for sustainable, safe, and cost-effective EES. However, attempts to use these materials for EES have so far led to subpar cycling stability and charging rates due to insufficient stability, low electrical conductivity, and reduced performance at commercial scales.

Metal-organic frameworks (MOFs) have the potential to rival or even supersede traditional EES materials. MOFs can be imbued with properties such as electronic conductivity by judicious design of their constituent building blocks. However, realizing the full potential of MOFs for EES requires joint expertise from distinct fields. Electrochemists and synthetic and materials chemists must work together to establish the unified approach necessary for achieving MOF-based EES devices with competitive performance.

Please cite this article in press as: Hong et al., Metal-organic frameworks for fast electrochemical energy storage: Mechanisms and opportunities, Chem (2023), https://doi.org/10.1016/j.chempr.2023.02.016

the formation of crystalline networks. The coordination geometry between metal node and ligand define the MOF's network topology and potential porosity.[14,15] The chemical identity of the nodes and ligands, along with MOF topology, plays a deterministic role in the ultimate functionality of the material. Many MOFs possess accessible porosity and high specific surface areas (SSAs)[16]; consequently, their applications in gas storage,[17] fluid separations,[18] and catalysis[19–22] have been extensively studied. MOFs designed for these applications typically feature metal ions bound with redox-inactive ligands via hard[23] coordinating motifs such as carboxylate[24] or imidazolate,[25] yielding robust, porous frameworks that however lack the electrical conductivity and redox activity necessary for fast EES.[26]

MOFs for fast EES must fulfill the set of stringent requirements outlined above to be competitive with (or superior to) state-of-the-art systems. Meeting these requirements necessitates an altogether different and distinct approach to MOF design. For example, learning from design principles of conductive coordination polymers, electrical conductivity can be introduced.[26,27] An emerging class of electrically conductive MOFs shows a marked improvement in performance over their non-conductive counterparts and demonstrates substantial promise for high-rate energy storage.[15,28] Along with electrical conductivity, density and accessibility of the redox-active sites and MOF stability under operating conditions are equally critical to consider at the design stage.

This review aims to bridge the knowledge gap between electrochemists and scientists working in the field of MOFs. We introduce basic concepts of energy storage devices and electrochemical characterization techniques. We then discuss design principles of MOFs in the context of what parameters are important to consider for their use in fast EES devices. Given the nascence of this field, many questions regarding energy storage mechanisms remain unaddressed, such as the effect of redox-active centers and porosity (e.g., size, shape, and pore volume) on device performance. Further, we identify opportunities for the rational design of MOFs for energy storage applications. For comprehensive reviews providing extensive assessments of the performance of MOF-based fast EES devices, the interested reader is directed to recent publications.[13,29–36]

FARADIC AND CAPACITIVE CHARGE STORAGE FOR FAST CHARGING

Knowledge of distinct charge storage mechanisms and understanding their advantages and drawbacks are critical to enable the design of next-generation energy storage materials.[37] Fundamental differences in the operation principles exist between faradic and non-faradic charge storage mechanisms (Figure 1). As the name suggests, the former involves redox reactions that follows Faraday's law (in bulk or at the surface of the material), while the latter is a redox-free physical mechanism termed electrical double-layer (EDL) capacitance.

The EDL mechanism relies on charge separation in the EDL upon polarization that is achieved through the reversible electrosorption of ions from the electrolyte to the outer and inner (from pores) surfaces of the material (Figure 1). Therefore, to maximize EDL capacitance, electrode materials with high SSA and good ionic accessibility are used. For example, highly porous carbons with SSA > 1,500 m^2/g demonstrate the highest EDL capacitances[37] and are used as active materials in commercial supercapacitors (also known as electrochemical capacitors and ultracapacitors).[37] As the EDL capacitance does not involve redox processes, this mechanism is inherently fast.[37] As a result, devices that use EDL capacitance to store

[1]Electrochemical Energy Systems Laboratory, Department of Mechanical and Process Engineering, ETH Zurich, 8092 Zurich, Switzerland

[2]Department of Chemistry, The University at Albany, State University of New York, Albany, NY 12222, USA

*Correspondence: jfeldblyum@albany.edu (J.I.F.), mlukatskaya@ethz.ch (M.R.L.)

https://doi.org/10.1016/j.chempr.2023.02.016

Please cite this article in press as: Hong et al., Metal-organic frameworks for fast electrochemical energy storage: Mechanisms and opportunities, Chem (2023), https://doi.org/10.1016/j.chempr.2023.02.016

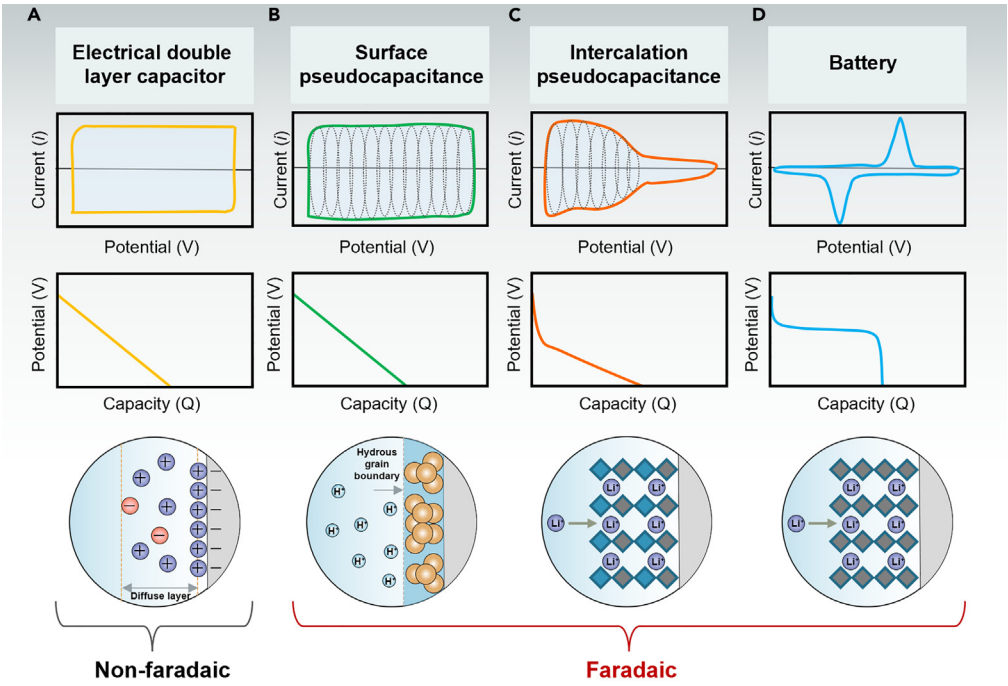

Figure 1. Faradic and capacitive charge storage

Characteristic cyclic voltammetry and galvanostatic profiles and schematic diagrams depicting characteristics of each charge storage mechanism: electrical double-layer capacitor (A), surface pseudocapacitance (B), intercalation pseudocapacitance (C), and battery (D). Figure adapted from Lukatskaya et al.[11] and Simon et al.[12]

charge (e.g., supercapacitors) benefit from fast charging and are characterized by high power operation and excellent cycling stability (>100,000 cycles).[37] EDL capacitors (EDLCs) are characterized by the rectangular shapes of their cyclic voltammograms (CVs) and linear galvanostatic charge-discharge profiles (Figure 1).

Electrode materials in batteries, on the other hand, rely on redox reactions to store charge (i.e., the operation mechanism is faradic), which are accompanied by ion insertion/intercalation and phase transformations.[2,11,37] Redox-based charge storage is characterized by large specific capacities and an order of magnitude higher energy densities, compared with supercapacitors. However, due to unavoidable phase transformations, the operation of battery materials is limited by solid-state diffusion[38] during charge/discharge cycling.[2,11,37] Furthermore, insufficient ionic and electronic conductivities of common battery electrode materials make them inherently slower than supercapacitors and impose limitations on the specific power achievable by batteries.[2,39] CVs of battery electrode materials are characterized by well-separated redox peaks, while galvanostatic charge-discharge profiles feature plateaus at the corresponding redox potentials. Performance trade-offs between supercapacitors and batteries can be visualized using Ragone plots that use specific energy and power as their corresponding x and y axes.[37]

Pseudocapacitors are a subclass of electrochemical capacitors that rely on fast redox reactions for charge storage. Their electrochemical features resemble those of EDLCs (Figure 1); however, unlike EDLCs, the charge storage mechanism in pseudocapacitors is faradic in nature, enabling pseudocapacitors to store 5–10 times more charge, compared with EDLCs. Depending on whether redox processes occur at the material surface or within the bulk, pseudocapacitance can be classified as surface

Please cite this article in press as: Hong et al., Metal-organic frameworks for fast electrochemical energy storage: Mechanisms and opportunities, Chem (2023), https://doi.org/10.1016/j.chempr.2023.02.016

redox or intercalation, respectively.[10,37] Both types are characterized by sloping galvanostatic charge-discharge profiles (Figure 1). Pseudocapacitors can potentially bridge the gap between batteries and EDLCs, with energy density approaching that of batteries and power densities reaching those of EDLCs. It is important to emphasize however a key difference between batteries and pseudocapacitors, as significant confusion exists in the literature: while both utilize faradic mechanisms, pseudocapacitors are characterized by fast-charging kinetics not limited by diffusion and do not undergo phase transformation during charge/discharge cycling.[11] Moreover, only a select few materials show true pseudocapacitive behavior, as they have to combine good electronic and ionic conductivity to display fast-charging kinetics.[10,12,40] Known examples of pseudocapacitive systems illustrate that ion transport to a redox-active site can be assisted by the presence of (1) structural solvent,[41] e.g., hydrated RuO_2[42] and 2D transition carbonitrides (MXenes),[11,43] or (2) low-barrier ion diffusion channels, such as in T-Nb_2O_5.[44]

The design of fast energy storage devices (that rely on the outlined mechanisms to store charge) requires an understanding and optimization of the many interdependent factors that ultimately define the final performance of the device. In the next section we introduce these factors.

BASIC CONCEPTS OF ENERGY STORAGE DEVICES

Factors affecting performance of the electrochemical energy storage device

Researchers in academia and industry alike target concurrent improvements in the specific energy, power, and durability of electrochemical EES devices, all while lowering their overall costs.[45,46] All of these device characteristics are typically presented as normalized by total device weight and volume. When comparing the performance and commercial viability of fast EES devices, it is important to take all these metrics into consideration.[45] EES devices are constructed from the following key components: (1) positive and negative electrodes that store charge, which are made of a mixture of active material, conductive additives (e.g., carbon black) that improve the electronic conductivity of the electrode, and a small amount of polymeric binder (typically PTFE [Polytetrafluoroethylene (Teflon)] or PVDF [Polyvinylidene fluoride]) that maintains the structural integrity of the electrode; (2) electrolyte whose function is to conduct ions; (3) a separator that prevents electrical contact and therefore short circuiting between the positive and negative electrodes; (4) current collectors that ensure electrical contact to the active material; and (5) device casing.[2,47,48] All these components contribute to overall device weight and volume and therefore the respective device metrics (outlined below).[48] Therefore, to achieve maximized performance, all device components and their relative ratios require special optimization.[48] In Figure 2, we depict the key aspects considered for device optimization at the electrolyte, electrode, and active materials levels, highlighting the interdependence of these factors on overall device performance.

Cost

While the topic of cost optimization is outside the scope of this review, in Figure 2 we list important factors that are known to affect the final device cost[49]: while element scarcity represents a foundational cost-determining parameter, supply chain efficiency and scalability of material production are equally important as they can directly affect the cost of the device.[48] Another parameter that is increasingly taken into consideration is related to the recyclability. An exponential increase in EES device usage must be followed by an exponential increase in the number of end-of-life EES devices that must be disposed or recycled in sustainable, cost-effective ways.[49,50]

Please cite this article in press as: Hong et al., Metal-organic frameworks for fast electrochemical energy storage: Mechanisms and opportunities, Chem (2023), https://doi.org/10.1016/j.chempr.2023.02.016

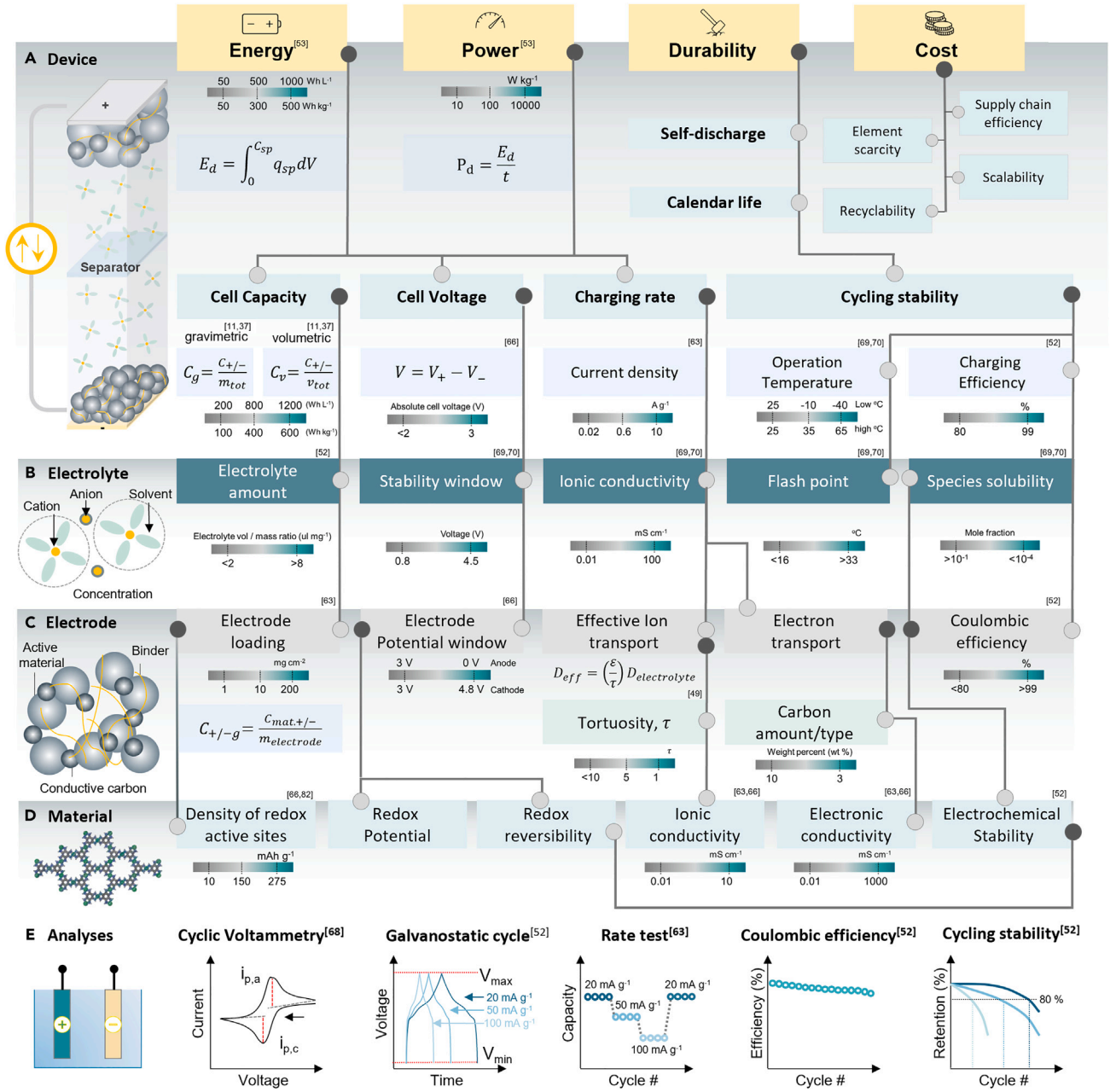

Figure 2. Energy storage device and material characteristics and relevant analyses

A guideline depicting the interconnected nature of how key characteristics of energy storage devices (A) are affected by electrolyte (B), electrode (C), and active material (D) selection, as well as typical electrochemical characterizations used to assess them (E). Connecting line scheme: filled dark gray symbols indicate that metrics are dependent on the parameter marked by the light gray symbol. Bar gradients provide reference values, where teal regions correspond to the most desirable range, while gray indicates less desirable values.

Durability

The number of cycles over which a fast EES device can be operated before losing 20% of its original performance (the cycle life) is one of the main metrics used to characterize the device durability.[51] Cycle life depends on the charge-discharge conditions (current density, cutoff voltages, and temperature) as these can directly affect Coulombic efficiency (CE) by prompting irreversible reactions associated with electrode and electrolyte decomposition (*vide infra*). To be competitive with other

Please cite this article in press as: Hong et al., Metal-organic frameworks for fast electrochemical energy storage: Mechanisms and opportunities, Chem (2023), https://doi.org/10.1016/j.chempr.2023.02.016

energy storage systems, at least 80% of the device capacity should be maintained after >1,000 cycles for batteries and >10,000 cycles for supercapacitors, respectively.[2,37,51,52] Other industry-relevant durability characteristics are self-discharge (characterized by the capacity loss with use)[37,53] and calendar life (measurement of capacity retention during a fixed period of time);[54,55] safety tests such as hot box test (thermal behavior monitoring under heating condition at 180°C)[56,57] and nail penetration test[58] (to simulate internal short circuit) are beyond the scope of this review.

Energy and fast-charging capability (power)

The specific energy of the device, W, is directly proportional to specific cell capacity, Q, (charge stored per total device volume or mass) and cell voltage V: $W = QV$ for a battery and $W = \frac{1}{2}QV$ for a supercapacitor.[59,60] Improving energy performance involves (1) maximizing the capacity of the positive and negative electrodes; (2) improving the volume and mass fractions of active charge storage material (e.g., higher electrode thicknesses/loadings), while reducing the fraction of inactive compounds (electrolyte, current collectors, and casing);[51,61] and (3) increasing the cell voltage.[51] The specific power of the device refers to its ability to deliver energy per unit of time and is proportional to energy density as a function of the charging rate (current density).[37] Specific power is affected by ion and electron transport within the electrodes and cell (*vide infra*).[10,37]

Capacity

For redox-based charge storage, electrode capacity primarily depends on the charge storage capability of the active material, i.e., the density of the redox-active sites per unit mass.[11,62] It can be estimated theoretically using the following equation: $Q_{theoretical}(mAh\ g^{-1}) = \frac{n \times F}{3.6\ W_F}$, where n is the number of electrons gained or lost by the material during charging per formula weight (W_F) of the active material, and F is the Faraday constant (96,485 C mol^{-1}).[2,10] The theoretical capacity can serve as a first benchmark to estimate whether a material might be attractive for energy storage applications. However, experimental values of specific capacity rarely reach theoretical values, in particular at high charging rates, due to the inherent difficulty of establishing excellent ion and electron accessibility at each redox-active site and/or due to the instability of the material after electrochemical cycling.[11] Therefore, materials for fast EES must have sufficiently high electronic conductivity. Furthermore, since most redox reactions require (de)insertion of ions to maintain charge balance, high ionic conductivities are also desirable in addition to a high density of redox-active sites.

Electrode loading

Effective ion transport and electronic conductivity are equally important at the electrode level. For practical cells it is critical to demonstrate the scalability of active material performance at industry-relevant loadings of >10 mg/cm^2.[63] Doing so necessitates inclusion of conductive additives (e.g., carbon black) for active materials possessing lower conductivity.[6] Generally, while having larger content of conductive additives improves power characteristics when normalized just per active material weight, when total electrode weight is considered, overall electrode capacity can drop.[11,63] Effective ion transport within the electrode is closely related to effective diffusivity that is a product of ion diffusivity within electrolyte and tortuosity: $D_{eff} = D_t$.[61] Tuning the tortuosity of the electrode will have significant impact on ionic transport.

Voltage

The difference between the positive and negative electrode potentials defines the cell voltage, and increasing the cell voltage constitutes one of the ways to improve

Please cite this article in press as: Hong et al., Metal-organic frameworks for fast electrochemical energy storage: Mechanisms and opportunities, Chem (2023), https://doi.org/10.1016/j.chempr.2023.02.016

the energy density of the device.[37] For redox-based energy storage, selection of positive and negative electrode materials that yield large differences between their reversible redox potentials is one of the ways to increase overall energy density.[64] To ensure high charging efficiencies, irreversible reactions at the electrodes (e.g., leaching of cations or ligands, structure collapse, and electrolyte decomposition) lead to loss of capacity with cycling and should be avoided.[6,10] In order to find out experimentally the *reversible* redox potential window for the active material, cycling voltammetry or galvanostatic cycling (GC) can be used in a three-electrode configuration (that allows for separately tracking electrochemical behavior of the material of interest).[65,66] Selection of positive and negative cutoff potentials can strongly affect the CE (defined as discharge capacity over charge capacity × 100) and cycle life (defined as the plot of discharge capacity with cycle number).[11,38,53] Therefore, tests with variable cutoff voltages should be conducted to identify the optimal potential range in which the active material experiences the least degradation.[53]

Electrolyte

Electrolyte selection affects cell performance on multiple levels: (1) To maximize energy density, the amount of electrolyte must be minimized while still ensuring proper electrode material wetting for optimal ion accessibility to active sites.[51] High ionic conductivity is necessary for fast charging (ensuring high rate performance and thus power).[67] (2) The voltage window in which the electrolyte is stable (as defined by the electrolyte's oxidation and reduction decomposition potentials) constitutes another critical parameter.[68] This voltage window is affected by solvent selection and electrolyte concentration.[68] Electrolytes based on organic solvents (e.g., acetonitrile or organic carbonates) and ionic liquids offer higher stability windows (>3 V), compared with water that has a thermodynamic stability window of 1.23 V.[69] To ensure high charging efficiency, the electrode redox potentials should fall within the electrolyte stability window. Otherwise, charge would be spent on electrolyte decomposition.[11] (3) The electrolyte flash point is an important safety characteristic, and its low values, as in the case of organic electrolytes, can lead to safety concerns and limit device operation temperatures.[67] (4) Electrolyte composition can also affect the chemical and electrochemical stabilities of the active material.[67] Careful selection of the electrolyte can help to suppress degradation and thus dramatically affects the cycle life of the device.[68] It is important therefore to first assess the performance of the material in a range of electrolytes.[68]

Electrochemical characterization of MOFs

Typical electrochemical characterization techniques for energy storage materials are CV,[70] GC, and electrochemical impedance spectroscopy (EIS)[71,72] (Figure 2E). For evaluating a MOF's redox potential and capacity, both CV and GC can be utilized. Information on the rate performance of the material can also be obtained from CV and GC by changing experimental conditions such as scan or charging rate. Testing with different cutoff potentials can provide insights into the electrochemical stability of the material by comparing CEs.[55,56] EIS can provide knowledge of the capacitive and resistive behaviors at the material and electrode levels.[55,72,73] Lastly, galvanostatic charge-discharge cycle testing is commonly used to evaluate the cycling stability of the electrode under constant current conditions.[55] For more comprehensive overviews, the interested reader might find several tutorial reviews[55,56,74,75] helpful. These works discuss the principles of these characterization methods, how information such as redox potential, capacity, resistance, etc. can be obtained experimentally, and different electrochemical cell configurations and their benefits and drawbacks.

Please cite this article in press as: Hong et al., Metal-organic frameworks for fast electrochemical energy storage: Mechanisms and opportunities, Chem (2023), https://doi.org/10.1016/j.chempr.2023.02.016

DESIGN OF MOFs FOR FAST ELECTROCHEMICAL ENERGY STORAGE

As was emphasized above, sufficient electronic and ionic conductivity, a high density of redox-active sites, and electrochemical stability are all necessary characteristics of next-generation materials for fast EES. MOFs can potentially fulfill all these criteria. Below, we outline how each of these desirable characteristics can be expressed in MOFs. The *a priori* design of MOFs for fast EES is challenging, and successful candidates have thus far been based on a narrow subset of possible conductive MOF candidates (*vide infra*). However, the parameter space for new MOF design is essentially limitless (Figure 3A). We provide our personal perspective on key design rules for new MOFs for fast EES, aiming both to increase the diversity of MOFs studied to this end and to improve their performance to an extent where they might achieve commercial relevance.

Redox characteristics

For pseudocapacitive behavior, maximizing the density of redox-active sites is important for high device performance. Achieving this aim requires careful consideration of several factors that are discussed below.

To a first approximation, extending ligand length without changing the ligand's symmetry or coordination motifs will lead to MOFs having larger pores, but otherwise identical topology.[81] The relevance of this paradigm has been confirmed for 2D conductive MOFs.[82] Larger pores result in higher accessible surface area (see below) and therefore can enable increased contributions from double-layer capacitance to charge storage. Furthermore, larger pores can provide improved ion accessibility to the redox-active sites critical for fast charging. Yet, despite the noted advantages of larger pores and higher accessible surface area (see below), such characteristics come at the cost of inherently reducing the volumetric density of redox-active sites in the MOF. Moreover, where ligand extension does not concomitantly include additional ligand-based redox states, the gravimetric density of redox-active sites is also reduced. Hence, smaller ligands generally lead to greater capacity as long as redox-active sites remain accessible.

The redox characteristics of both metal and ligand are also important for maximizing the density of redox-active sites within the MOF. Both the ligand and metal (or metal cluster) should ideally be redox active and contribute to charge storage to maximize energy density. This aim can be achieved by redox matching, where both transition metal and ligand are redox-active in the same potential range.[83] While redox matching has been cited as enabling high conductivity in conductive MOFs,[84] direct evidence for matching ligand and metal redox potentials is still lacking. In fact, several authors have shown that pseudocapacitance in several 2D MOFs used for fast EES is ligand-centered.[85–87] The discovery of redox-matched motifs can be aided by the study of small-molecule coordination complexes having metal-ligand binding motifs analogous to those used to construct MOFs. Electrochemical studies of such complexes are amenable to solution-based spectroscopy methods to assess oxidation state changes in metal and ligand.[28,84,88] For example, a model tri-nickel hexaoxytriphenylene (HOTP) complex, used as an analog for the conductive MOF $Ni_3(HOTP)_4$, exhibits well-defined redox waves during electrochemical cycling.[88] A combination of CV and electron paramagnetic resonance (EPR) spectroscopy was used to show that redox is ligand-centered, with the oxidation state of Ni^{2+} remaining unchanged. *In situ* X-ray absorption spectroscopy (XAS) can be used to determine whether changes in metal oxidation state occur at potentials identical to those at which ligand oxidation state changes are detected (discussed below).

Please cite this article in press as: Hong et al., Metal-organic frameworks for fast electrochemical energy storage: Mechanisms and opportunities, Chem (2023), https://doi.org/10.1016/j.chempr.2023.02.016

CellPress

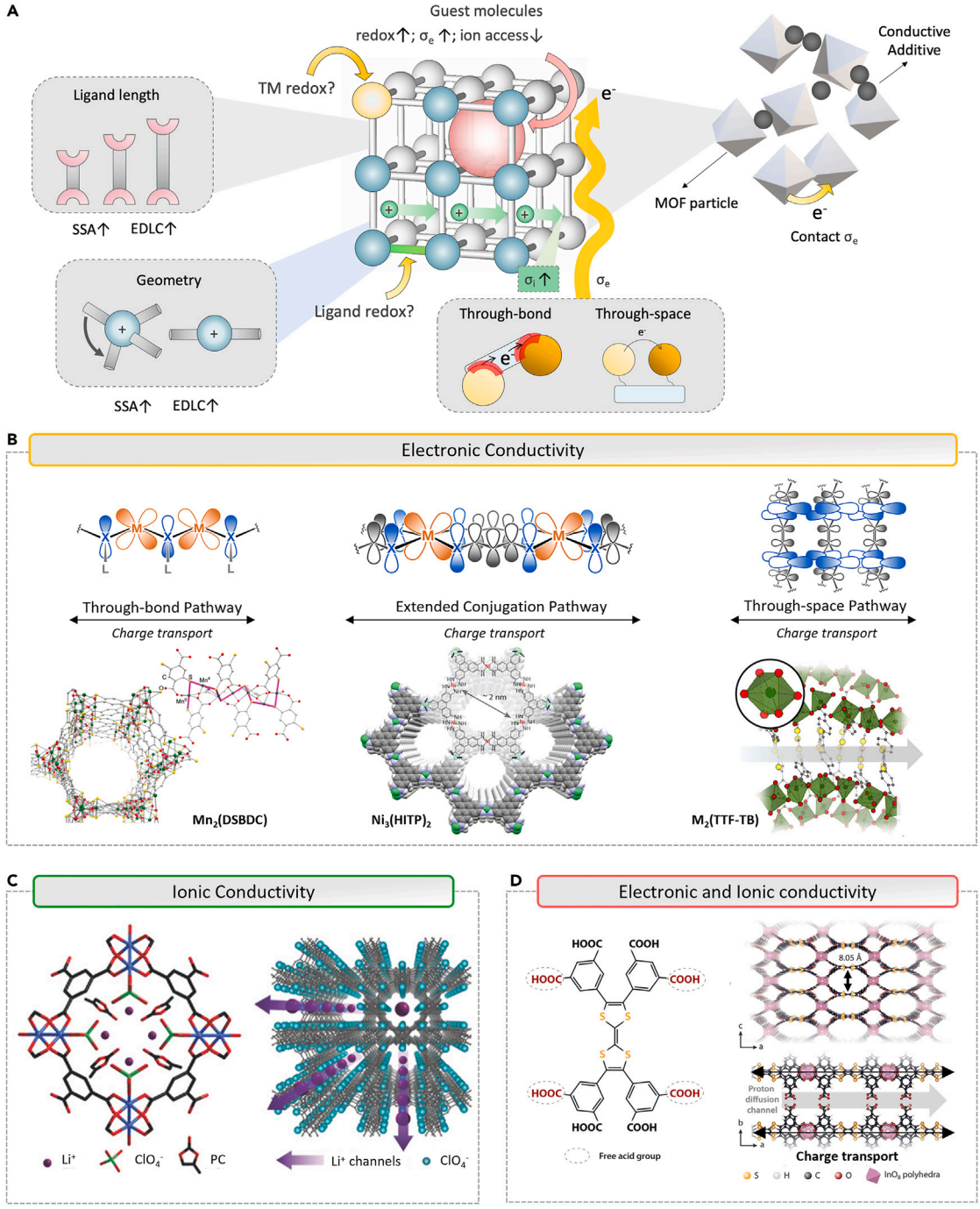

Figure 3. Relationships between electrochemical properties and MOF structure

(A and B) Schematic diagram (A); examples of high electrical conductivity MOFs with extended 2D conjugation (B).[26,76–78] Reprinted with permission from Xie et al.[26] Copyright 2020 American Chemical Society. Reprinted with permission from Park et al.[76] Copyright 2018 American Chemical Society. Reprinted with permission from Kirlikovali et al.[77] Copyright 2022 American Chemical Society. Reprinted with permission from Sun et al.[78] Copyright 2013 American Chemical Society.

(C) An example of a Li^+ conductive membrane using HKUST-1 with Li^+ and ClO_4^- bound to the open metal sites.[79] Reprinted with permission from Shen et al.[79] Copyright 2018 Wiley.

(D) Tetrathiafulvalene octacarboxylic acid forming 2D sheets that have both electrical and ionic conductivity.[80] Reprinted with permission from Kharod et al.[80] Copyright 2022 Annual Reviews.

Please cite this article in press as: Hong et al., Metal-organic frameworks for fast electrochemical energy storage: Mechanisms and opportunities, Chem (2023), https://doi.org/10.1016/j.chempr.2023.02.016

It is important to keep in mind that changes in the metal oxidation state can lead to changes in coordination geometry and therefore structural changes. Hence, structural characterization (e.g., via powder X-ray diffraction [PXRD]) of MOFs before and after cycling, and in each accessible redox state, is necessary to determine whether structural changes do in fact occur upon cycling and if they do, whether or not they are reversible (see below).

As discussed earlier, the energy density of a device is not only proportional to electrode capacity but also to cell voltage. Hence, the redox potential(s) of a MOF must be considered during its design. To maximize cell voltage, the redox potentials of the MOF-based anode material should be minimized and those of the cathode material maximized (as discussed above). Since MOFs consist of inorganic and organic components, the potential ranges of both the ligand and metal redox activity strongly depend on their respective identities. The redox potentials for ligands and transition metals, determined computationally (by density functional theory [DFT])[6,11] or experimentally (by CV),[28,70] can serve as starting points for the expected range of redox activity of the parent MOF. It is important to be cognizant of the fact that MOF assembly from these components can change these redox potentials. For example, even if the transition metal does not directly participate in charge storage, it can still influence the potentials at which ligand redox occurs in the MOF.[28] DFT calculations can be useful to pre-screen the relative effects of metal-ligand coordination on redox potentials that might ultimately be observed in the related MOFs. Finally, the redox potential of the MOF must lie within the electrochemical stability window of the electrolyte to achieve stable cycling.

Electronic conductivity

MOFs used for fast EES must have sufficient electronic conductivity. MOFs were initially designed with metal-ligand motifs that are unlikely to support conduction (e.g., cyano-metal[89] or carboxylate-metal[90] links), but in 2009, the first MOF with substantial guest-independent conductivity (6×10^{-4} S cm^{-1} at 300 K) was reported.[91] Since then, a diverse set of 2D and 3D MOFs has been discovered with conductivities up to and even exceeding 10^3 S cm^{-1}.[26] Several design strategies have been developed to produce conductive MOFs; these have been divided into through-bond, extended conjugation, and through-space approaches (Figure 3B, each described below).[26] Through-bond conjugated MOFs possess unbroken chains consisting of metal cations and ligand heteroatoms (typically N or S) that serve as conduction pathways. The carbonaceous ligand cores are assumed to not participate in electrical conduction. It is important to note that favorable energetic overlap between metal and heteroatom orbitals is necessary to enable effective charge delocalization along such chains. Through-bond MOFs featuring metal cations with adjacent oxidation states (e.g., Fe^{2+}/Fe^{3+}) constitute a special case where an additional boost to conductivity can be delivered. For example, Fe_2(1,4-benzenedipyrazolate)$_3$[92] has a conductivity of 10^{-2} S cm^{-1} [93]; allowing partial oxidation of the Fe^{2+} cations to Fe^{3+} in air increases the conductivity by two orders of magnitude.[94]

Extended conjugation refers to the case where charge delocalization is established between conjugated ligands and metal nodes. Similar to MOFs with through-bond conduction, good geometric and energetic orbital overlap between metal ions and non-innocent (redox-active) ligands is essential to achieving satisfactory conductivity.[26] Examples include MOFs that showed promising performance for fast EES, based on conjugated ligands having multiple *ortho*-dithiol, -diamine, or -diol groups bound to transition metal ions (noting that the metal does not necessarily contribute

Please cite this article in press as: Hong et al., Metal-organic frameworks for fast electrochemical energy storage: Mechanisms and opportunities, Chem (2023), https://doi.org/10.1016/j.chempr.2023.02.016

significantly to charge storage—*vide infra*). However, there is no fundamental reason why other MOFs with conductivity originating from through-bond interactions or extended conjugation could not also be deployed for fast EES. For example, an iron-based triazolate MOF showed substantial conductivity and mixed iron redox states,[95] but studies using this MOF for fast EES have not yet been reported. While the pores of this specific MOF are relatively small (ca. 4.5 Å), the use of extended triazole ligands could allow electrolyte ions access to the interior of the MOF without compromising conductivity. The synthesis and structures of numerous other 3D conductive MOFs that could potentially be promising for fast EES have been detailed;[22,26] however, their electrochemical performance has not been described.

MOFs with through-space conductivity possess conjugated organic ligands that are not covalently bound to one another but interact electronically via through-space π-orbital overlap. The iconic series of M_2(ttftb) MOFs (ttftb, tetrathiafulvalene-tetrabenzoate) is exemplary of this mode of conduction, where conductivity originates from π-π interactions between stacked ligands.[96] To date, however, conductivities in through-space conductive MOFs have been modest, typically not exceeding 10^{-2} S cm^{-1}.[26] It is possible that introducing donor-acceptor motifs akin to those found in charge-transfer salts[97] may produce through-space conductive MOFs with substantially higher conductivity, but this strategy currently poses significant synthetic challenges. Finally, through-space conductivity in MOFs can be introduced by guest molecules such as tetracyanoquinodimethane (tcnq).[98]

It is our current perspective that MOFs based on through-bond and extended conjugation conduction will remain the best performers for fast EES due to their reproducibly high conductivities (achievable without limiting porosity), but improvements in through-space conductive MOF design[26] may also lead to promising candidates for fast EES. Guest infiltration to enhance MOF redox characteristics and/or conductivity inherently limits ion access to pores and therefore, in our view, is unlikely to compete with current state-of-the-art materials. Finally, it is critical to remember that theoretical capacity estimates (described above) should serve as a guide for the selection of promising motifs that introduce electrical conductivity in a MOF.

Ionic conductivity

Ionic conductivity is a critical parameter for both pseudocapacitive and EDLC charge storage. To take full advantage of charge storage sites throughout the *volume* of the MOF (not just the MOF particle surface), ionic conductivity *within* the MOF must be sufficient (Figure 3C). To date, the strategies used to render MOFs ionically conductive are focused on achieving high proton conductivity; the conduction of other ions more relevant for energy storage (e.g., Li^+, Na^+, Mg^{2+}, etc.) is less studied. To achieve internal ionic conductivity, MOF linkers are typically decorated with acidic functional groups (e.g., carboxylic, sulfonic, or phosphonic acids)[80]—these functional groups can be added pre-synthetically (where they are part of the linker used to construct the MOF) or post-synthetically (where the MOF linkers are functionalized after the MOF is formed). While the former case can be more straightforward and does not suffer from sub-quantitative functionalization yield, the proclivity of acidic functional groups to coordinate directly to metal cations can lead to interference with MOF formation, rendering pre-synthetic functionalization challenging in some cases.[99] Conduction of other cations can be achieved by replacing acidic protons with larger cations (e.g., Li^+, Na^+, Mg^{2+}, etc.).[80] For MOFs with open metal sites (native to the MOF or introduced via defects,[100] e.g., as in the accessible Cr cations in MIL-101[101]), ion conduction can be introduced by functionalization of these sites.[102] Ionic conductivity in MOFs can emerge after infiltration with liquid

Please cite this article in press as: Hong et al., Metal-organic frameworks for fast electrochemical energy storage: Mechanisms and opportunities, Chem (2023), https://doi.org/10.1016/j.chempr.2023.02.016

electrolyte. Finally, for MOFs with sufficiently large pores, both electrolyte ions and solvent are expected to populate these pores, in which case ionic conductivity originates solely from electrolyte confined in the MOF pores.[103]

For MOFs with smaller pores, the correlation between a MOF's ionic conductivity and its pore size is not well established due to the difficulty of decoupling the effects of pore size and the distance between ion hopping sites. In a recent report, the proton conductivity was greater for a smaller-pore MOF compared with a larger-pore analog.[103] While this report of smaller pores yielding superior H^+ conductivity is consistent with previous observations for Li^+,[104] the opposite trend was observed for Mg^{2+}.[105] Furthermore, the effect of dimensionality on ionic conduction has to our knowledge lacked systematic study, but using MOFs having 3D pore networks could also improve ion transport, compared with MOFs having 1D channel pores of the same size.

Electronic conductivity is also a critical factor for a MOF's utility for fast EES, but few MOFs with simultaneous ionic and electronic conductivity have been reported.[106,107] A possible strategy to obtain such dual-conducting MOFs would be to incorporate moieties known to support ion conduction (described above) into electronically conductive MOFs. However, it is critical to consider the negative effects of introducing redox-inactive moieties on theoretical and experimental capacity (Figure 3D).

IMPLICATIONS OF SYNTHESIS ON MOF PROPERTIES

The size and crystallinity of MOF particles can strongly affect the electrochemical response of MOF-based electrodes. For ionically and electronically conductive MOFs, higher crystallinity is desirable. Larger MOF crystalline domains will result in higher intraparticle electronic conductivity. However, if larger crystalline domains have insufficient ionic conductivity, charge storage will be limited by solid-state ion diffusion. Thus, for MOFs with poor ionic conductivity, smaller particle sizes can enable faster charging via increased accessibility to redox-active sites by electrolyte ions. Meanwhile, for MOFs with high ionic (greater than that of the ionic conductivity of the electrolyte) and electronic conductivity (higher than that of conductive additives, e.g., carbon black), electrodes with smaller particles will display lower conductivity due to the increased role of interparticle transport, negatively affecting the overall charging rates. Computational modeling have been utilized to explore the effect of different MOF properties (e.g., pore size, SSA, and particle size)[13,108,109] on capacitance and performance; future studies in this area are expected to provide further data for how such properties influence energy storage device characteristics.

Control over particle size and crystallinity

The formation of extended coordination networks (MOFs) from ligand and transition metal occurs via their *reversible* ligand-metal coordination. Upon dissolution, both ligand and transition metal cation are solvated by solvent molecules and/or counterion. Therefore, MOF formation process in solution is strongly affected by solvent identity (and especially whether solvent(s) are protic or aprotic, or basic or acidic), reagent selection (i.e., counterion of the transition metal salt or ligand protonation) and concentration, the presence (or absence) of assisting agents such as modulators and co-solvents, and impurities (e.g., residual water). Each of these parameters as well as reaction temperature can additionally tune the rate of network formation and hence MOF crystallinity and particle size. If the rate of MOF formation is too high, the quality/crystallinity of the product can suffer.[110] Hence, numerous

Please cite this article in press as: Hong et al., Metal-organic frameworks for fast electrochemical energy storage: Mechanisms and opportunities, Chem (2023), https://doi.org/10.1016/j.chempr.2023.02.016

strategies that enable the control of crystallization have been developed: (1) ligands are typically introduced in protonated form; their deprotonation, required to realize the ligand-metal coordination that drives MOF assembly, is enabled by introduction of base. Examples include *N*,*N*-dimethylformamide (DMF) that serves both as a solvent and a base,[111] organic amines (e.g., triethylamine),[112] and inorganic base (e.g., aqueous NH_3).[113] The strength of the base and its rate of introduction can both impact the product characteristics: slower rates tend to yield higher-quality (e.g., more crystalline) MOFs.[114,115] (2) Various modulators can be used to suppress MOF nucleation and slow crystallite growth. Modulators are small molecules (e.g., ethylenediamine[116]) or anionic species (e.g., benzoate[117]) that compete with the ligand for transition metal cation coordination, thereby reducing the rate at which these cations can participate in MOF formation. Modulators have previously proven to be effective to enable the growth of single crystals instead of micro- or nanocrystalline powders of network materials.[118,119] (3) Higher temperatures (ca. 60°C–120°C) can assist in MOF crystallization; however, it is essential to understand that increasing the reaction temperature can change the thermodynamically favorable phase, potentially yielding undesirable products.[120]

Defects

Despite the apparent simplicity of solvothermal synthesis, the morphology, crystal structure, and even chemical composition can be extremely sensitive to synthesis conditions. For example, the Dincă group showed that apart from parameters discussed above, experimental variables such as exposure to air vs. inert environment and even the volume of the reaction flask influence the aspect ratio of the formed MOF.[121] Despite the importance of experimental parameters on the outcome of synthesis, there are few systematic studies exploring this subject.[122] Thus, several precautions should be taken when attempting to reproduce a MOF synthesis from the literature or synthesize a new MOF. Changes in reaction conditions (e.g., solvent, temperature, and time) can result in significant changes in network topology.[123] Moreover, defects can play an important role in MOF porosity, pore size, and access to potentially redox-active metal nodes.[124] Defects can be introduced (or avoided) by using modulators—typically HCl or capping ligands of coordination chemistry similar to that of the ligands used to form the MOF itself.[124,125] Handling and treatment of MOFs post-synthesis is also important. For example, pore (and structure) collapse upon guest removal[126] or even solvent exchange[127] can occur. Hence, caution should be applied when drying MOFs prior to or after electrode fabrication, as this process may lead to structure changes such as intralayer displacement or structural collapse[128]; these changes may be detected by PXRD and gas sorption analysis.

New MOFs

When synthesis of new MOFs is pursued, several principles can be applied. Transition metal coordination and ligand geometries can dictate MOF structure. To this end, existing MOFs can be useful to inform how components with similar geometries might self-assemble. However, as discussed above, practical realization of such *a priori* prediction of MOF structure can be challenged by the complex solution chemistry that drives MOF phase selection (e.g., counterions and solvent molecules can incorporate into the MOF structure, leading to the formation of unexpected MOF phases). If no relevant references are available, the following experimental parameters can serve as reasonable starting points: DMF as a solvent, temperatures of 25°C and 100°C (temperatures commonly used for successful MOF synthesis), the presence or absence of water (which may influence the crystallinity of the resulting

Please cite this article in press as: Hong et al., Metal-organic frameworks for fast electrochemical energy storage: Mechanisms and opportunities, Chem (2023), https://doi.org/10.1016/j.chempr.2023.02.016

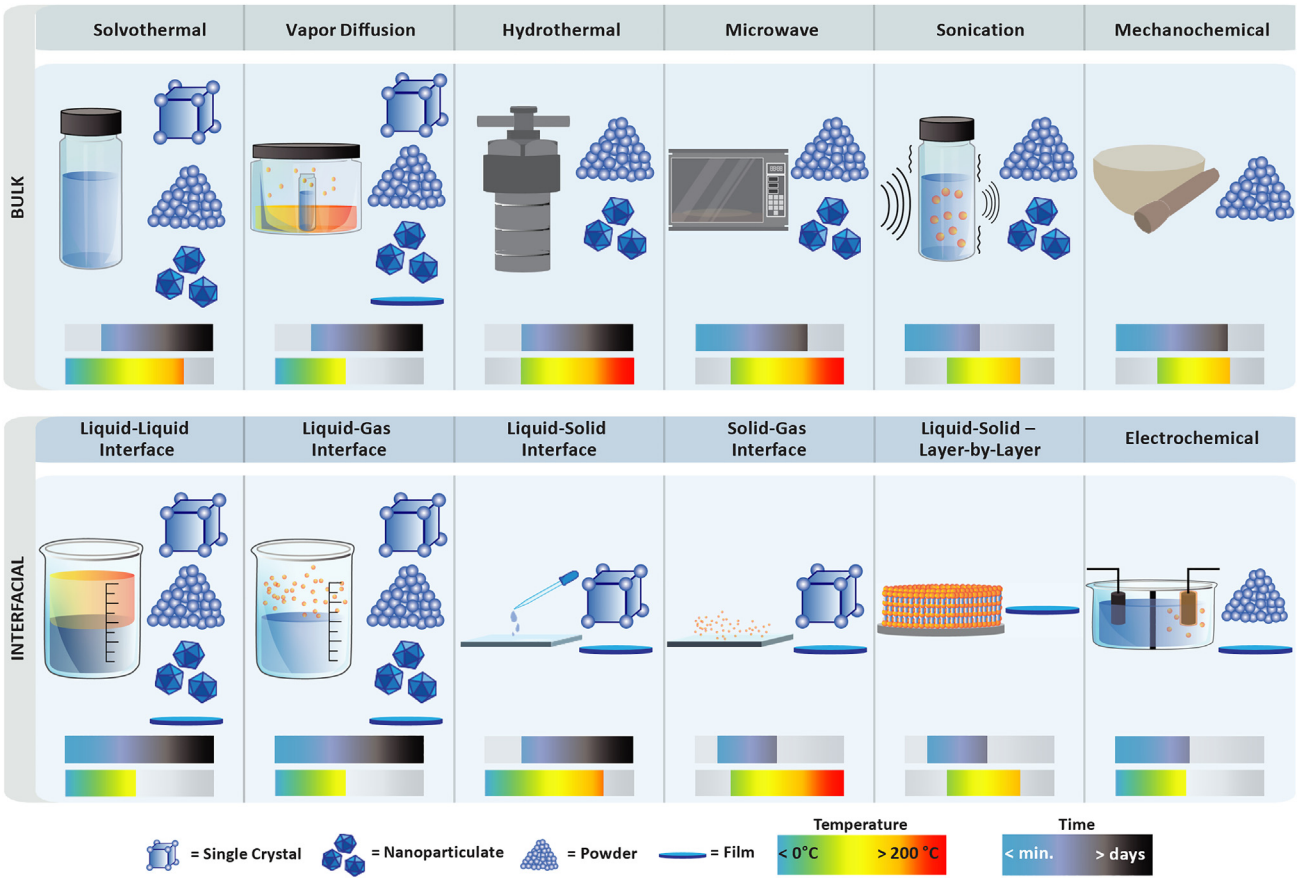

Figure 4. Common approaches to MOF synthesis

Schematic illustration of common approaches to MOF synthesis and their respective typical reaction temperatures, times, and MOF product morphologies.

MOF),[114] and the inclusion (or absence) of common modulators such as sodium acetate.[129]

Many approaches exist to synthesize MOFs; these are summarized in Figure 4. It is recommended to begin by choosing a method that does not prevent obtaining a MOF with the desired particle size and morphology (e.g., nanocrystalline powder, single crystal, or film). While micro- or even nanocrystalline MOF powders are most often used for fast EES devices, obtaining MOFs as films directly on current collectors may be beneficial (e.g., for micro-supercapacitors).[130]

CHARACTERIZATION OF MOFs

Structure and morphology

MOFs are crystalline materials, and diffraction methods therefore form the basis for their characterization (Figure 5). New MOFs for fast EES generally possess strong metal-ligand coordination bonds of low kinetic reversibility, making it especially difficult to obtain crystals of a size and quality suitable for single-crystal X-ray diffraction (Figure 5A). Therefore, structure solution from high-resolution, synchrotron-based X-ray diffraction of powder samples is often a necessary starting point to elucidate their structures. Structure solution from powder diffraction is rarely straightforward, and available methods generally require at least a moderate level of expertise in both the powder diffraction theory and appropriate software (the

Please cite this article in press as: Hong et al., Metal-organic frameworks for fast electrochemical energy storage: Mechanisms and opportunities, Chem (2023), https://doi.org/10.1016/j.chempr.2023.02.016

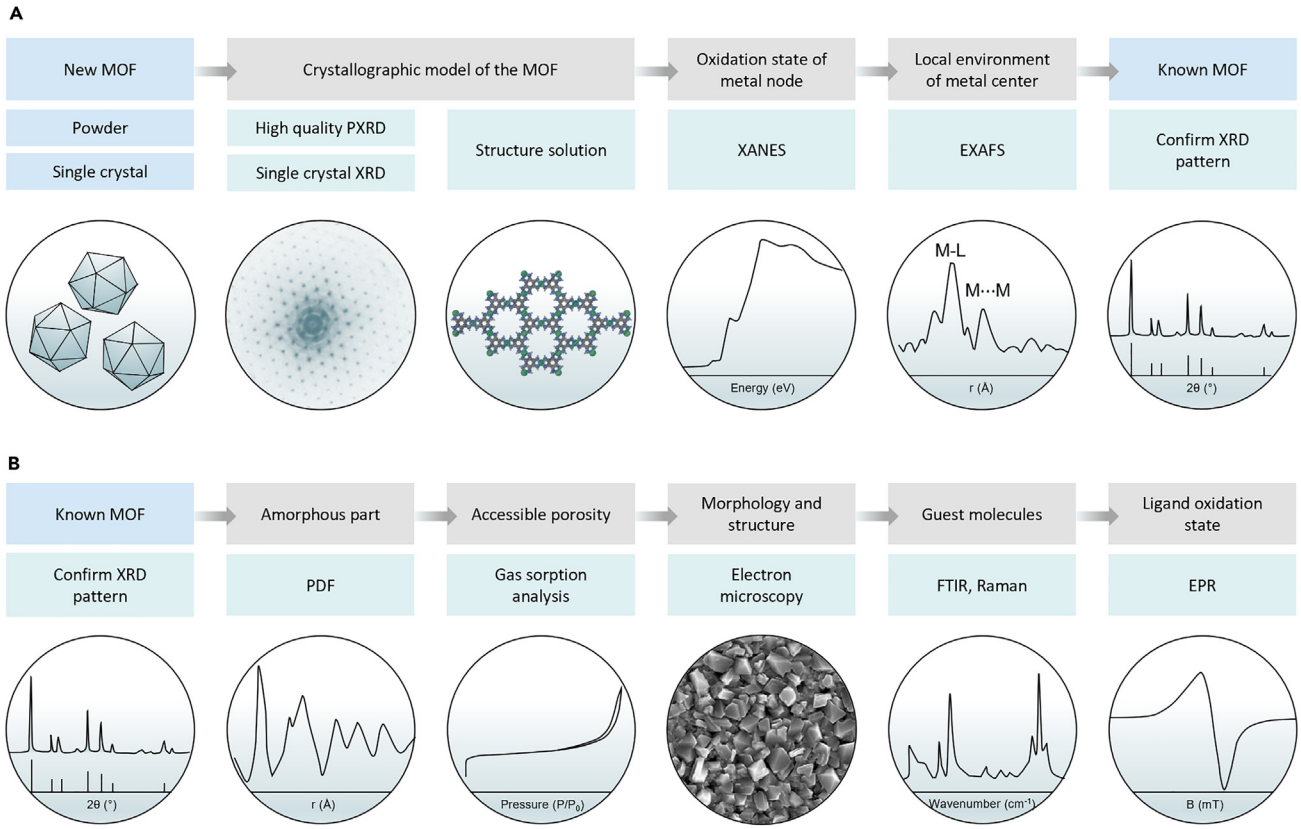

Figure 5. Characterization of MOFs

Characterization algorithm for new (A) and known (B) MOFs to assist with comprehensive characterization of their structure and properties.

interested reader is referred to a recent review on the subject and references therein).[131] *In situ* optical methods such as dark-field microscope (DFM) can be used to trace the evolution of MOFs crystal growth.[132] Transmission electron microscopy (TEM) imaging and electron diffraction enables analysis of the smaller crystallites as well as can provide information about secondary or amorphous phases.[133] However, due to the sensitive nature of MOF samples, it is essential to ensure that the sample does not undergo beam damage during data acquisition. To do so, a low-dose TEM approach is applied.[134] In cases where the structure of the MOF is known, PXRD is used to confirm the identity of synthesis products. This is generally a far more straightforward process, whereby standard laboratory X-ray diffractometers are sufficient for data collection, and data analysis typically involves a simple visual comparison of peak positions and intensities. Rietveld refinement provides a more quantitative and reliable approach to confirm phase identity but is rarely carried out in practice. For example, Rietveld refinement can be used to quantify potential differences in stacking modes and intralayer stacking distances for 2D MOFs.[135,136] The pair distribution function obtained from diffuse scattering data can be used to describe the atom-atom distances of the sample and therefore captures the structure of any amorphous phase present.[137] Amorphous regions typically lack the high porosity of the intended crystalline phase[138] and complicate interpretation of electrochemical data (for example, determining to what extent *internal* redox-active sites are electrochemically accessible). Finally, we stress that the crystallinity of the MOF should be assessed both before *and* after operation in an electrochemical device: MOFs may be sensitive to exposure to the conditions

Please cite this article in press as: Hong et al., Metal-organic frameworks for fast electrochemical energy storage: Mechanisms and opportunities, Chem (2023), https://doi.org/10.1016/j.chempr.2023.02.016

needed to operate fast EES devices, and observed device performance may be related to the MOF degradation products rather than to the MOF itself. Even post-synthesis treatments such as guest exchange, guest removal, and temperature changes can influence the MOF's structure,[138] so analytical data before and after such changes is necessary to ensure that the structure of the synthesized MOF is retained when used as an electrode material.

The crystallographic model of a MOF belies the complexity that is possible with experimental MOF samples. Synthesized MOFs can contain a wide variety of irregularities including surface defects, missing linkers, or nodes, occluded guests (solvent, counterions, metal salts, etc.), stacking faults, non-uniform metal oxidation states and coordination environments, and differences in particle morphology. All these irregularities can dramatically impact the characteristics of the experimental sample. For example, accessible internal surface area and pore size can both be increased[139] or decreased[140] by structural defects, and occluded guests and stacking faults usually prevent access by ions (with exceptions[86,141]). We emphasize here that *the basic characterization of MOFs solely by X-ray diffraction is entirely insufficient to reveal these irregularities and that these irregularities are fundamental to the performance of MOFs in fast EES devices*. We provide here several examples that describe the analytical techniques used to identify the important characteristics of experimentally obtained samples (Figure 5B).

Gas sorption is typically used to measure SSA[142] and pore size distribution. The SSA derived from gas sorption measurements can under- or overestimate the electrochemically active surface area, since ion intercalation kinetics is a complex function of pore characteristics (size, shape, and chemistry), potential for intercalation,[86] and solvent. Furthermore, gas sorption is best suited for the characterization of micro- and mesopores, doing a poor job of capturing macroporosity and >100-nm-scale surface roughness that can impact electrochemical behavior.[143] Pore size distributions are obtained from DFT fits that are designed for traditional sorbents such as activated carbons and zeolites. Hence, pore size distributions derived from applying these models to experimental gas sorption data can potentially be quite inaccurate and provide little insight into whether the MOF's internal pores play a significant role in electrochemical behavior. A combination of gas sorption and electrochemically active surface area measurements (see below) is recommended to provide a more complete picture of the role porosity plays in the electrochemical behavior of the MOF.

Chemistry

Measurements with X-ray absorption near-edge spectroscopy (XANES) and extended X-ray absorption fine structure (EXAFS) can be used to determine the metal oxidation states and coordination number, respectively,[144] the latter potentially hinting at coordinated guests that are not part of the crystallographic model or stacking faults present between sheets in 2D MOFs.[145] For example, EXAFS analysis of the conductive 2D MOF $Ni_3(HITP)_2$ (HITP = 2,3,6,7,10,11-hexaiminotriphenylene) was used to show, on the basis of Ni–Ni distances, that a slipped-parallel best characterizes interlayer stacking.[146] The stacking mode is critical: staggered geometries can render potential pores inaccessible, preventing ion ingress and egress and thereby hindering electrochemical device performance.[133] Furthermore, these techniques can be used *in situ* during energy device cycling. For example, XANES was used to show that the metal oxidation state of Ni_3(hexaaminobenzene)$_2$ does not participate in redox processes during pseudocapacitive operation, indicating that changes in oxidation state are fully attributable to the non-innocent ligands within the material.[85] Once the structure of the MOF is known, EPR can be used to provide

Please cite this article in press as: Hong et al., Metal-organic frameworks for fast electrochemical energy storage: Mechanisms and opportunities, Chem (2023), https://doi.org/10.1016/j.chempr.2023.02.016

insights into the electronic states of the MOF. For non-innocent ligands, EPR can establish the presence of radicals (or lack thereof) and assist in the determination of their oxidation states. However, as it is very sensitive to the presence of unpaired electrons, it should be coupled with other techniques to definitively establish the electronic states present in the MOF.[147]

The morphology of synthesized MOFs is well known to have a strong impact on the fabrication and behavior of MOF-based electrodes. Scanning electron microscopy (SEM) is generally the most straightforward way to determine MOF particle size and shape. The researcher must however obtain statistically relevant sample sizes and use image processing software to determine particle dimension and aspect ratio computationally to reduce user bias where possible. Care should also be taken when interpreting particle size data in that the observed particle size does not necessarily reflect the crystallite size.

The chemical purity of MOFs should be assessed by several analytical approaches. Since most MOFs are porous, the chemical contents of these compounds changes with the contents of the pores themselves. To circumvent this complication, the MOF must be "activated" prior to chemical analysis: activation typically involves rinsing the MOF several times with polar and non-polar solvents and then heating the MOF under reduced pressure for several hours to days.[126] The MOF should then be subjected to elemental (CHN, and other elements where applicable) analysis and inductively coupled plasma mass spectrometry (ICP-MS) or optical emission spectroscopy (ICP-OES) to determine the metal content.[148] These techniques together show whether the expected chemical formula accurately describes the synthesized material. Nuclear magnetic resonance (NMR), infrared spectroscopy, and Raman spectroscopy can be used to detect occluded or trapped guests. Taking advantage of NMR for MOF chemical analysis typically requires digestion (dissociative dissolution) of the MOF in an appropriate deuterated solvent. The often modest solubility of the linkers used to form the MOF can pose a challenge. Hence, experimentation with digestion solutions to ensure complete dissolution of the MOF is often necessary. Good starting points for this experimentation can be strongly acidic solutions (e.g., trifluoroacetic acid, concentrated HCl), strongly basic solutions (e.g., aqueous or DMF solutions of NaOH), and others.[149]

UNDERSTANDING OF CHARGE STORAGE MECHANISM AND DEGRADATION

It is essential to understand the charge storage and degradation mechanism of MOF electrodes. This knowledge can provide important guidelines toward improving the performance of existing systems as well as insight into the design of next-generation MOF-based high-performance electrodes. In Figure 6, we depict a set of characterization guidelines that can assist in determining the dominant storage mechanisms. Below, we discuss the advantages and challenges associated with the use of each technique. As a first step, the contribution of the double-layer capacitance (F/g) can be estimated based on the accessible surface area,[85] using the following equation: $C_{dl} = C_A \cdot A$, where C_A is the areal capacitance (typically in the range between 5 and 20 $\mu F/cm^2$, depending on the solvent and material; for an upper-bound estimate, higher values of ~20 $\mu F/cm^2$ can be used for conductive MOFs)[85] and A is the SSA (m^2/g) that can be obtained from gas sorption analysis.[142] If the estimated C_{dl} value is much lower than the capacitance calculated from the electrochemical measurements, it can serve as a clear indicator that other mechanisms (i.e., pseudocapacitance) are at play.[11,44]

Please cite this article in press as: Hong et al., Metal-organic frameworks for fast electrochemical energy storage: Mechanisms and opportunities, Chem (2023), https://doi.org/10.1016/j.chempr.2023.02.016

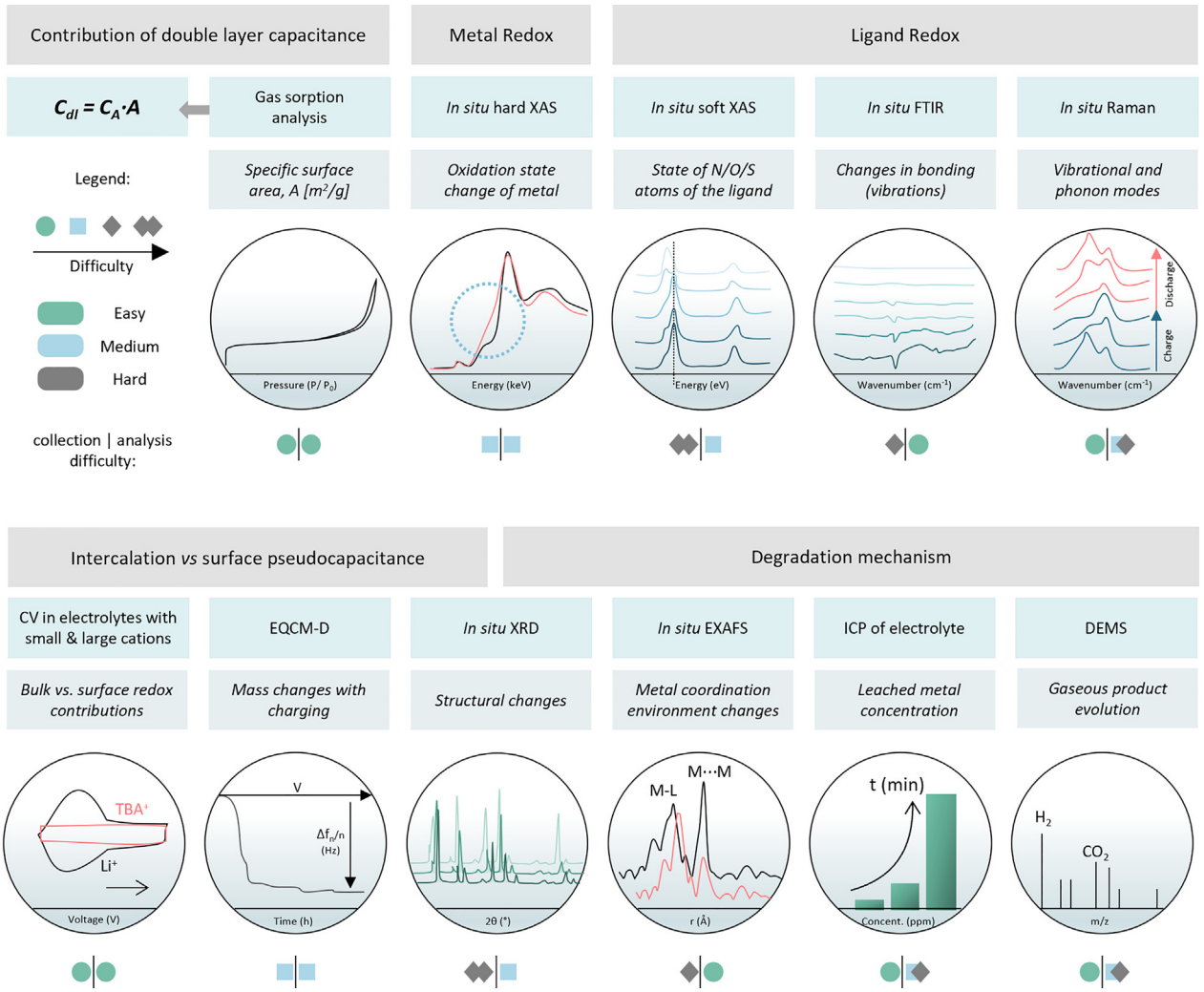

Figure 6. Assessment of charge storage and degradation mechnisms in MOFs

Characterization methodology (light teal boxes) to assist in deriving the dominant electrochemical charge storage and degradation mechanisms in MOFs (gray boxes).

To gain insights into the contributions of the ligand and transition metal redox to charge storage, changes in their respective oxidation states have to be monitored during charge/discharge.[85] For example, using *in situ* hard XAS one can quantify the valence change of the transition metal by tracking changes in its edge energy.[150,151] Furthermore, analysis of the EXAFS region coupled with *in situ* XRD can provide important information about the reversibility of the changes in the transition metal coordination environment as a function of cycling and applied potential.[21,151,152] Insights into potential electrochemistry-induced degradation pathways can also be extracted from such measurements.[153] As discussed above, ligand redox can also significantly contribute to charge storage. However, quantitative assessment of its role in charge storage is not always easy. While *in situ* XAS can provide quantitative information regarding changes in the ligand's oxidation state, soft X-rays must be used to probe light atoms such as C, O, N, and S.[154,155] Due to the strong absorption of soft X-rays by most materials,[150] the measurement setup should be designed to minimize the loss of X-ray intensity due to absorption by the electrolyte or window material or even gas atmosphere.[150] Therefore, soft

Please cite this article in press as: Hong et al., Metal-organic frameworks for fast electrochemical energy storage: Mechanisms and opportunities, Chem (2023), https://doi.org/10.1016/j.chempr.2023.02.016

XAS has to be collected using specialized experimental configurations that feature electrochemical cells with SiN or SiC membrane windows at the working electrode that allow transmission of the soft X-rays.[150,156] These configurations should also include gas-free paths for emitted X-rays to the detector.[150]

Due to pronounced experimental challenges related to *in situ* XAS methodology, *ex situ* XAS (both hard and soft X-ray) and XPS measurements are used at different states of charge.[85,157] However, it is important to keep in mind the risks related to self-discharge during sample preparation that can result in underestimation of the metal/ligand redox contribution.[158] Therefore, in most cases, other *in situ* techniques must be utilized in tandem to provide insights into ligand redox. Thus, *in situ* Raman spectroscopy is another widely used method to analyze the chemical state of the organic ligand during charging.[85] For instance, the evolution of the benzene-ring-related vibrations at different charge/discharge states was established by *in situ* Raman spectroscopy, revealing the reduction of the ligand within the MOF structure.[85] However, it is important to note that exact assignment of Raman peaks is not trivial and in many cases requires DFT calculations[159] or information from prior experiments with ligands that have been deuterated to assist with peak assignment.[160]

By contrast, Fourier transform infrared spectroscopy (FTIR) can offer direct information about the chemical state of the ligand at different states of charge.[161] For example,[161,162] using *in situ* FTIR, it was revealed that reversible reduction of carbonyl groups in the poly(anthraquinonyl sulfide)-based cathode is accompanied by insertion of cations (Li^+ or Mg^{2+}) during charge storage, and it has also revealed the further formation of the intermediate semiquinone radical anions.[161] However, to mitigate interfering spectroscopic signatures of the solvent/electrolyte, such *in situ* FTIR studies must be performed using reflection or thin-layer cell geometry.[161,163] For *ex situ* FTIR, the standard approach to preparing samples involving dilution in KBr pellets can easily disrupt the metastable charged state of MOF ligand (i.e., self-discharge)[161] and therefore yield misleading results. Meanwhile, the use of pure MOF pellets can result in low-quality FTIR data.

Distinguishing the intercalation and surface pseudocapacitance mechanisms can be achieved by several methods. First and perhaps the most straightforward approach entails comparing MOF capacitance obtained in electrolytes containing alkylammonium cations larger than the MOF pores with that obtained in electrolytes with smaller cations such as Li^+ or Na^+.[44,85] Capacitance values that do not differ significantly are indicative of surface, rather than intercalation, pseudocapacitance. As cation insertion can lead to changes in MOF lattice parameters, coupling such measurements with *in situ* XRD can yield further insights into structural changes (and their reversibility) that the MOF may experience during charging.[164] Another technique that can provide important mechanistic insight is electrochemical quartz crystal microbalance (EQCM) measurements that can track mass changes at the electrodes upon charging.[165] Quantitative information can be extracted about species entering the electrode material during charging by correlating electrode mass changes with the mass of the charge carrier ion. Thus, EQCM can be used to reveal the charge carrier ion's solvation state upon entering the pores of the electrode.[166]

Understanding MOF degradation pathways is the key to engineering MOF-based electrodes with a long cycle life.[26] The chemical instability of MOFs in certain environments (e.g., electrolytes) is typically caused by competition between ligand, solvent, and/or anion for coordination to the metal center.[167] As of now, an understanding of the electrochemically driven degradation of MOFs is lacking. However,

Please cite this article in press as: Hong et al., Metal-organic frameworks for fast electrochemical energy storage: Mechanisms and opportunities, Chem (2023), https://doi.org/10.1016/j.chempr.2023.02.016

presumably, much like for inorganic materials,[2] the electrochemical instability of MOFs originates when the coordination between metal and ligand is compromised by metal or ligand redox processes,[167,168] leading to cumulative structural degradation of the MOF upon repetitive cycling.[168,169] The roles of solvent and salt selection can be critical to the electrochemical degradation rate, hence optimal choice of solvent and salt can assist with stabilization of the structure.[170,171] *In situ* XAS and XRD can help to reveal changes in metal site coordination, irreversible structural changes of the electrode material, and formation of secondary phases.[155,172] MOF collapse, which also results in transition metal leaching from the electrode, can be tracked via time-dependent analysis of transition metal concentration in electrolyte, using ICP analysis.[173] As previously noted, electrolyte decomposition can also result in poor cycling stability. Differential electrochemical MS (DEMS) can be used to track the formation of gaseous products (e.g., H_2, CO, CO_2, and O_2) that are associated with electrolyte decomposition.[174,175]

OUTLOOK

In this review, we outlined MOF design principles for fast EES and highlighted the importance of gaining insights into MOF charge storage mechanisms. Significant progress has been made in recent years in the area of MOF-based EES devices, especially with the introduction of electrically conductive MOFs. However, we see numerous directions in need of concerted efforts from both MOF chemists and electrochemists to further advance this field and render MOF-based EES devices competitive with or better than traditional inorganic-based energy storage electrodes.

First, thus far, most of the promising examples of MOF-based energy storage are of MOF-based negative electrodes (anodes). Meanwhile, the field of MOF-based cathodes remains in its infancy primarily due to the lack of conductive MOFs that are reversibly redox active at higher potentials. Hence, new MOFs are needed that simultaneously incorporate redox moieties active in the potential range > 3 V vs. Li/Li^+ and that can also deliver high capacities.

Second, to date, most conductive MOFs display ligand-based redox, while transition metal cations have not directly contributed to charge storage during EES device cycling. Hence, to yield further improvements in achievable pseudocapacitance, it is necessary to redox-match transition metals with their partner ligands, which may require exploration of MOF architectures that have received little attention for fast EES to date (for example, 3D conductive MOFs). The study of small-molecule coordination complexes (as discussed above) can assist in selecting metal-ligand motifs that support redox matching in analogous MOFs. DFT simulations can further accelerate the discovery of promising motifs by rapid screening[176] for robust redox matching.

Third, past work examining the behavior of carbide-derived carbons with uniform pore size has shown that double-layer capacitance is maximized when the pore size matches the size of the infiltrating organic ion.[177] We foresee that MOFs can also benefit from enhanced EDL capacitance if MOF pore size is matched to the size of the solvated ions. This can be achieved by systematically changing the MOF's ligand length without changing the ligand geometry (see above).[81]

Finally, as cycle life is critical for fast EES, it is important to achieve MOF electrode cycling stability over at least several thousand cycles. To this end, the mechanisms by which MOFs electrochemically degrade, and the role of electrolyte in MOF degradation, must be better understood.

ACKNOWLEDGMENTS

C.N.H. and M.R.L. acknowledge support from the ReMaP project, funded by the Swiss Federal Office of Energy under contract SI/501810-01 and the ETH Foundation. A.B.C. and J.I.F. acknowledge support from the Donors of the American Chemical Society Petroleum Research Fund (no. 59835-DNI10) and startup funds from the University at Albany, SUNY in support of this work. We also thank Dr. Evgeniya Vorobyeva for her help in shaping the initial draft of this manuscript.

AUTHOR CONTRIBUTIONS

Conceptualization, M.R.L. and J.I.F.; investigation, M.R.L., J.I.F., C.N.H., and A.B.C.; visualization, M.R.L., J.I.F., C.N.H., and A.B.C.; funding acquisition, M.R.L. and J.I.F.; project administration, M.R.L. and J.I.F.; supervision, M.R.L. and J.I.F.; writing – original draft, M.R.L., J.I.F., C.N.H., and A.B.C.; writing – review & editing, M.R.L., J.I.F., C.N.H., and A.B.C.

DECLARATION OF INTERESTS

The authors declare no competing interests.

REFERENCES

1. Dell, R.M., and Rand, D.A.J. (2001). Energy storage — a key technology for global energy sustainability. J. Power Sources *100*, 2–17.
2. Abakumov, A.M., Fedotov, S.S., Antipov, E.V., and Tarascon, J.M. (2020). Solid state chemistry for developing better metal-ion batteries. Nat. Commun. *11*, 4976.
3. Zeng, A., Chen, W., Rasmussen, K.D., Zhu, X., Lundhaug, M., Müller, D.B., Tan, J., Keiding, J.K., Liu, L., Dai, T., et al. (2022). Battery technology and recycling alone will not save the electric mobility transition from future cobalt shortages. Nat. Commun. *13*, 1341.
4. Usiskin, R., Lu, Y., Popovic, J., Law, M., Balaya, P., Hu, Y.-S., and Maier, J. (2021). Fundamentals, status and promise of sodium-based batteries. Nat. Rev. Mater. *6*, 1020–1035.
5. Lee, S., Kwon, G., Ku, K., Yoon, K., Jung, S.K., Lim, H.D., and Kang, K. (2018). Recent progress in organic electrodes for Li and Na rechargeable batteries. Adv. Mater. *30*, 1704682.
6. Lu, Y., and Chen, J. (2020). Prospects of organic electrode materials for practical lithium batteries. Nat. Rev. Chem. *4*, 127–142.
7. Min, X., Xiao, J., Fang, M., Wang, W., Zhao, Y., Liu, Y., Abdelkader, A.M., Xi, K., Kumar, R.V., and Huang, Z. (2021). Potassium-ion batteries: outlook on present and future technologies. Energy Environ. Sci. *14*, 2186–2243.
8. Kwabi, D.G. (2021). Molecular engineering expands the chemical possibilities for organic flow batteries. Joule *5*, 1636–1638.
9. Vorobyeva, E., Lissel, F., Salanne, M., and Lukatskaya, M.R. (2021). Bottom-up design of configurable oligomer-derived conducting metallopolymers for high-power electrochemical energy storage. ACS Nano *15*, 15422–15428.
10. Fleischmann, S., Mitchell, J.B., Wang, R., Zhan, C., Jiang, D.E., Presser, V., and Augustyn, V. (2020). Pseudocapacitance: from fundamental understanding to high power energy storage materials. Chem. Rev. *120*, 6738–6782.
11. Lukatskaya, M.R., Dunn, B., and Gogotsi, Y. (2016). Multidimensional materials and device architectures for future hybrid energy storage. Nat. Commun. *7*, 12647.
12. Simon, P., Gogotsi, Y., and Dunn, B. (2014). Materials science. Where do batteries end and supercapacitors begin? Science *343*, 1210–1211.
13. Niu, L., Wu, T., Chen, M., Yang, L., Yang, J., Wang, Z., Kornyshev, A.A., Jiang, H., Bi, S., and Feng, G. (2022). Conductive metal-organic frameworks for supercapacitors. Adv. Mater. *34*, e2200999.
14. Robson, R. (2000). A net-based approach to coordination polymers. J. Chem. Soc. Dalton Trans. 3735–3744.
15. Kim, J., Kim, Y., Yoo, J., Kwon, G., Ko, Y., and Kang, K. (2022). Organic batteries for a greener rechargeable world. Nat. Rev. Mater. *8*, 54–70.
16. Hönicke, I.M., Senkovska, I., Bon, V., Baburin, I.A., Bönisch, N., Raschke, S., Evans, J.D., and Kaskel, S. (2018). Balancing mechanical stability and ultrahigh porosity in crystalline framework materials. Angew. Chem. Int. Ed. Engl. *57*, 13780–13783.
17. Millward, A.R., and Yaghi, O.M. (2005). Metal−organic frameworks with exceptionally high capacity for storage of carbon dioxide at room temperature. J. Am. Chem. Soc. *127*, 17998–17999.
18. Li, J.R., Sculley, J., and Zhou, H.C. (2012). Metal–organic frameworks for separations. Chem. Rev. *112*, 869–932.
19. Pascanu, V., González Miera, G., Inge, A.K., and Martín-Matute, B. (2019). Metal–organic frameworks as catalysts for organic synthesis: A critical perspective. J. Am. Chem. Soc. *141*, 7223–7234.
20. Zhou, Z., Kong, Y., Tan, H., Huang, Q., Wang, C., Pei, Z., Wang, H., Liu, Y., Wang, Y., Li, S., et al. (2022). Cation-vacancy-enriched nickel phosphide for efficient electrosynthesis of hydrogen peroxides. Adv. Mater. *34*, e2106541.
21. Zhao, S., Tan, C., He, C.-T., An, P., Xie, F., Jiang, S., Zhu, Y., Wu, K.-H., Zhang, B., Li, H., et al. (2020). Structural transformation of highly active metal–organic framework electrocatalysts during the oxygen evolution reaction. Nat. Energy *5*, 881–890.
22. Qin, Y., Li, Z., Duan, Y., Guo, J., Zhao, M., and Tang, Z. (2022). Nanostructural engineering of metal-organic frameworks: construction strategies and catalytic applications. Matter *5*, 3260–3310.
23. Pearson, R.G. (1969). Hard and soft acids and bases. Surv. Prog. Chem. *5*, 1–52.
24. Li, H.E., Eddaoudi, M., Groy, T.L., and Yaghi, O.M. (1998). Establishing microporosity in open metal-organic frameworks: gas sorption isotherms for Zn(BDC) (BDC = 1,4-benzenedicarboxylate). J. Am. Chem. Soc. *120*, 8571–8572.
25. Huang, X.C., Lin, Y.Y., Zhang, J.P., and Chen, X.M. (2006). Ligand-directed strategy for zeolite-type metal-organic frameworks: zinc(II) imidazolates with unusual zeolitic topologies. Angew. Chem. Int. Ed. Engl. *45*, 1557–1559.
26. Xie, L.S., Skorupskii, G., and Dincă, M. (2020). Electrically conductive metal–organic frameworks. Chem. Rev. *120*, 8536–8580.
27. Fan, K., Zhang, C., Chen, Y., Wu, Y., and Wang, C. (2021). The chemical states of

conjugated coordination polymers. Chem *7*, 1224–1243.

28. Feng, D., Lei, T., Lukatskaya, M.R., Park, J., Huang, Z., Lee, M., Shaw, L., Chen, S., Yakovenko, A.A., Kulkarni, A., et al. (2018). Robust and conductive two-dimensional metal−organic frameworks with exceptionally high volumetric and areal capacitance. Nat. Energy *3*, 30–36.

29. Liu, J., Song, X., Zhang, T., Liu, S., Wen, H., and Chen, L. (2021). 2D conductive metal–organic frameworks: an emerging platform for electrochemical energy storage. Angew. Chem. Int. Ed. Engl. *60*, 5612–5624.

30. Wang, D.-G., Liang, Z., Gao, S., Qu, C., and Zou, R. (2020). Metal-organic framework-based materials for hybrid supercapacitor application. Coord. Chem. Rev. *404*, 213093.

31. Xu, B., Zhang, H., Mei, H., and Sun, D. (2020). Recent progress in metal-organic framework-based supercapacitor electrode materials. Coord. Chem. Rev. *420*, 213438.

32. Zhan, F., Wang, H., He, Q., Xu, W., Chen, J., Ren, X., Wang, H., Liu, S., Han, M., Yamauchi, Y., and Chen, L. (2022). Metal–organic frameworks and their derivatives for metal-ion (Li, Na, K and Zn) hybrid capacitors. Chem. Sci. *13*, 11981–12015.

33. Zhu, B., Wen, D., Liang, Z., and Zou, R. (2021). Conductive metal-organic frameworks for electrochemical energy conversion and storage. Coord. Chem. Rev. *446*, 214119.

34. Chu, J., Wang, Y., Zhong, F., Feng, X., Chen, W., Ai, X., Yang, H., and Cao, Y. (2021). Metal/covalent-organic frameworks for electrochemical energy storage applications. EcoMat *3*, e12133.

35. Guo, Y., Wang, K., Hong, Y., Wu, H., and Zhang, Q. (2021). Recent progress on pristine two-dimensional metal–organic frameworks as active components in supercapacitors. Dalton Trans. *50*, 11331–11346.

36. Li, W., Zhao, X., Bi, Q., Ma, Q., Han, L., and Tao, K. (2021). Recent advances in metal–organic framework-based electrode materials for supercapacitors. Dalton Trans. *50*, 11701–11710.

37. Simon, P., and Gogotsi, Y. (2020). Perspectives for electrochemical capacitors and related devices. Nat. Mater. *19*, 1151–1163.

38. Lim, J., Li, Y., Alsem, D.H., So, H., Lee, S.C., Bai, P., Cogswell, D.A., Liu, X., Jin, N., Yu, Y.S., et al. (2016). Origin and hysteresis of lithium compositional spatiodynamics within battery primary particles. Science *353*, 566–571.

39. Winter, M., and Brodd, R.J. (2004). What are batteries, fuel cells, and supercapacitors? Chem. Rev. *104*, 4245–4269.

40. Gogotsi, Y., and Penner, R.M. (2018). Energy storage in nanomaterials - capacitive, pseudocapacitive, or battery-like? ACS Nano *12*, 2081–2083.

41. Boyd, S., Ganeshan, K., Tsai, W.Y., Wu, T., Saeed, S., Jiang, D.E., Balke, N., van Duin, A.C.T., and Augustyn, V. (2021). Effects of interlayer confinement and hydration on capacitive charge storage in birnessite. Nat. Mater. *20*, 1689–1694.

42. Zheng, J.P.C., Cygan, P.J., and Jow, T.R. (1995). Hydrous ruthenium oxide as an electrode material for electrochemical capacitors. J. Electrochem. Soc. *142*, 2699–2703.

43. Anasori, B., Lukatskaya, M.R., and Gogotsi, Y. (2017). 2D metal carbides and nitrides (MXenes) for energy storage. Nat. Rev. Mater. *2*, 16098.

44. Augustyn, V., Come, J., Lowe, M.A., Kim, J.W., Taberna, P.L., Tolbert, S.H., Abruña, H.D., Simon, P., and Dunn, B. (2013). High-rate electrochemical energy storage through Li^+ intercalation pseudocapacitance. Nat. Mater. *12*, 518–522.

45. Schmuch, R., Wagner, R., Hörpel, G., Placke, T., and Winter, M. (2018). Performance and cost of materials for lithium-based rechargeable automotive batteries. Nat. Energy *3*, 267–278.

46. Mann, M., Babinec, S., Putsche, V., Hendrickson, S., Ho, H., Spitsen, P., Feldman, D., Gilleran, S.G.M., Hunter, C., Penev, M., et al. (2020). Energy storage grand challenge: energy storage market report (United States Department of Energy). https://www.energy.gov/sites/prod/files/2020/12/f81/Energy%20Storage%20Market%20Report%202020_0.pdf.

47. Simon, P., and Gogotsi, Y. (2008). Materials for electrochemical capacitors. Nat. Mater. *7*, 845–854.

48. Palacin, M.R. (2021). Battery materials design essentials. Acc. Mater. Res. *2*, 319–326.

49. Baum, Z.J., Bird, R.E., Yu, X., and Ma, J. (2022). Lithium-ion battery recycling—overview of techniques and trends. ACS Energy Lett. *7*, 712–719.

50. Harper, G., Sommerville, R., Kendrick, E., Driscoll, L., Slater, P., Stolkin, R., Walton, A., Christensen, P., Heidrich, O., Lambert, S., et al. (2019). Recycling lithium-ion batteries from electric vehicles. Nature *575*, 75–86.

51. Xiao, J., Li, Q., Bi, Y., Cai, M., Dunn, B., Glossmann, T., Liu, J., Osaka, T., Sugiura, R., Wu, B., et al. (2020). Understanding and applying coulombic efficiency in lithium metal batteries. Nat. Energy *5*, 561–568.

52. Harlow, J.E., Ma, X., Li, J., Logan, E., Liu, Y., Zhang, N., Ma, L., Glazier, S.L., Cormier, M.M.E., Genovese, M., et al. (2019). A wide range of testing results on an excellent lithium-ion cell chemistry to be used as benchmarks for new battery technologies. J. Electrochem. Soc. *166*, A3031–A3044.

53. Zhang, S., Ma, J., Hu, Z., Cui, G., and Chen, L. (2019). Identifying and addressing critical challenges of high-voltage layered ternary oxide cathode materials. Chem. Mater. *31*, 6033–6065.

54. de Biasi, L., Schwarz, B., Brezesinski, T., Hartmann, P., Janek, J., and Ehrenberg, H. (2019). Chemical, structural, and electronic aspects of formation and degradation behavior on different length scales of Ni-Rich NCM and Li-Rich HE-NCM cathode materials in Li-ion batteries. Adv. Mater. *31*, e1900985.

55. Hunt, G. (1996). Electric vehicle battery test procedures manual (Idaho National Engineering Laboratory). https://avt.inl.gov/sites/default/files/pdf/battery/usabc_manual_rev2.pdf.

56. Hou, J., Jang, W., Kim, S., Kim, J.H., and Byun, H. (2018). Rapid formation of polyimide nanofiber membranes via hot-press treatment and their performance as Li-ion battery separators. RSC Adv. *8*, 14958–14966.

57. Orendorff, C.J., Joshua, L., and Steele, L.A.M. (2015). FY 2014 annual progress report for energy storage R&D (Sandia National Laboratory). https://www.energy.gov/sites/prod/files/2015/04/f21/FY2014_APR_Energy_Storage_R%26D_FINAL_Part1_of_3.pdf.

58. Louli, A.J., Eldesoky, A., Weber, R., Genovese, M., Coon, M., deGooyer, J., Deng, Z., White, R.T., Lee, J., Rodgers, T., et al. (2020). Diagnosing and correcting anode-free cell failure via electrolyte and morphological analysis. Nat. Energy *5*, 693–702.

59. Abruña, H.D., Kiya, Y., and Henderson, J.C. (2008). Batteries and electrochemical capacitors. Phys. Today *61*, 43–47.

60. Conway, B.E. (1999). Electrochemical Supercapacitors: Scientific Fundamentals and Technological Applications (Kluwer Academic).

61. Kuang, Y., Chen, C., Kirsch, D., and Hu, L. (2019). Thick electrode batteries: principles, opportunities, and challenges. Adv. Energy Mater. *9*, 1901457.

62. Park, J.-K. (2012). Principles and Applications of Lithium Secondary Batteries (Wiley-VCH Verlag & Co. KGaA).

63. Gogotsi, Y.S., and Simon, P. (2011). Materials science. True performance metrics in electrochemical energy storage. Science *334*, 917–918.

64. Goodenough, J.B., and Kim, Y. (2010). Challenges for rechargeable Li batteries. Chem. Mater. *22*, 587–603.

65. Talaie, E., Bonnick, P., Sun, X., Pang, Q., Liang, X., and Nazar, L.F. (2017). Methods and protocols for electrochemical energy storage materials research. Chem. Mater. *29*, 90–105.

66. Yang, X., and Rogach, A.L. (2019). Electrochemical techniques in battery research: a tutorial for nonelectrochemists. Adv. Energy Mater. *9*, 1900747.

67. Xu, K. (2004). Nonaqueous liquid electrolytes for lithium-based rechargeable batteries. Chem. Rev. *104*, 4303–4417.

68. Xu, K. (2014). Electrolytes and interphases in Li-ion batteries and beyond. Chem. Rev. *114*, 11503–11618.

69. Shen, Y., Liu, B., Liu, X., Liu, J., Ding, J., Zhong, C., and Hu, W. (2021). Water-in-salt electrolyte for safe and high-energy aqueous battery. Energy Storage Mater. *34*, 461–474.

70. Elgrishi, N., Rountree, K.J., McCarthy, B.D., Rountree, E.S., Eisenhart, T.T., and Dempsey, J.L. (2018). A practical beginner's guide to cyclic voltammetry. J. Chem. Educ. *95*, 197–206.

71. Wang, S., Zhang, J., Gharbi, O., Vivier, V., Gao, M., and Orazem, M.E. (2021). Electrochemical impedance spectroscopy. Nat. Rev. Methods Primers *1*, 41.

72. Gaberšček, M. (2021). Understanding Li-based battery materials via electrochemical impedance spectroscopy. Nat. Commun. *12*, 6513.

73. Taberna, P.L., Simon, P., and Fauvarque, J.F. (2003). Electrochemical characteristics and impedance spectroscopy studies of carbon-carbon supercapacitors. J. Electrochem. Soc. *150*, A292.

74. Mathis, T.S., Kurra, N., Wang, X., Pinto, D., Simon, P., and Gogotsi, Y. (2019). Energy storage data reporting in perspective—guidelines for interpreting the performance of electrochemical energy storage systems. Adv. Energy Mater. *9*, 1902007.

75. Murray, V., Hall, D.S., and Dahn, J.R. (2019). A guide to full coin cell making for academic researchers. J. Electrochem. Soc. *166*, A329–A333.

76. Park, J.G., Aubrey, M.L., Oktawiec, J., Chakarawet, K., Darago, L.E., Grandjean, F., Long, G.J., and Long, J.R. (2018). Charge delocalization and bulk electronic conductivity in the mixed-valence metal-organic framework fe(1,2,3-triazolate)$_2$(BF$_4$)$_x$. J. Am. Chem. Soc. *140*, 8526–8534.

77. Kirlikovali, K.O., Goswami, S., Mian, M.R., Krzyaniak, M.D., Wasielewski, M.R., Hupp, J.T., Li, P., and Farha, O.K. (2021). An electrically conductive tetrathiafulvalene-based hydrogen-bonded organic framework. ACS Mater. Lett. *4*, 128–135.

78. Sun, L., Miyakai, T., Seki, S., and Dincă, M. (2013). Mn$_2$(2,5-disulfhydrylbenzene-1,4-dicarboxylate): a microporous metal-organic framework with infinite (-Mn-S-)$_\infty$ chains and high intrinsic charge mobility. J. Am. Chem. Soc. *135*, 8185–8188.

79. Shen, L., Wu, H.B., Liu, F., Brosmer, J.L., Shen, G., Wang, X., Zink, J.I., Xiao, Q., Cai, M., Wang, G., et al. (2018). Creating lithium-ion electrolytes with biomimetic ionic channels in metal-organic frameworks. Adv. Mater. *30*, e1707476.

80. Kharod, R.A., Andrews, J.L., and Dincă, M. (2022). Teaching metal-organic frameworks to conduct: ion and electron transport in metal-organic frameworks. Annu. Rev. Mater. Res. *52*, 103–128.

81. Abrahams, B.F.H., Hoskins, B.F., Michail, D.M., and Robson, R. (1994). Assembly of porphyrin building blocks into network structures with large channels. Nature *369*, 727–729.

82. Yao, M.S., Wang, P., Gu, Y.F., Koganezawa, T., Ashitani, H., Kubota, Y., Wang, Z.M., Fan, Z.Y., Otake, K.I., and Kitagawa, S. (2021). A comparative study of honeycomb-like 2D π-conjugated metal–organic framework chemiresistors: conductivity and channels. Dalton Trans. *50*, 13236–13245.

83. Kingsborough, R.P., and Swager, T.M. (1998). Electroactivity enhancement by redox matching in cobalt salen-based conducting polymers. Adv. Mater. *10*, 1100–1104.

84. Sun, L., Campbell, M.G., and Dincă, M. (2016). Electrically conductive porous metal–organic frameworks. Angew. Chem. Int. Ed. Engl. *55*, 3566–3579.

85. Lukatskaya, M.R., Feng, D., Bak, S.M., To, J.W.F., Yang, X.Q., Cui, Y., Feldblyum, J.I., and Bao, Z. (2020). Understanding the mechanism of high capacitance in nickel hexaaminobenzene-based conductive metal–organic frameworks in aqueous electrolytes. ACS Nano *14*, 15919–15925.

86. Banda, H., Dou, J.H., Chen, T., Zhang, Y., and Dincă, M. (2021). Dual-ion intercalation and high volumetric capacitance in a two-dimensional non-porous coordination polymer. Angew. Chem. Int. Ed. Engl. *60*, 27119–27125.

87. Zhang, P., Wang, M., Liu, Y., Yang, S., Wang, F., Li, Y., Chen, G., Li, Z., Wang, G., Zhu, M., et al. (2021). Dual-redox-sites enable two-dimensional conjugated metal-organic frameworks with large pseudocapacitance and wide potential window. J. Am. Chem. Soc. *143*, 10168–10176.

88. Yang, L., and Dincă, M. (2021). Redox ladder of Ni$_3$ complexes with closed-shell, mono-, and diradical triphenylene units: molecular models for conductive 2D MOFs. Angew. Chem. Int. Ed. Engl. *60*, 23784–23789.

89. Hoskins, B.F.R., and Robson, R. (1989). Infinite polymeric frameworks consisting of three dimensionally linked rod-like segments. J. Am. Chem. Soc. *111*, 5962–5964.

90. Yaghi, O.M.L., Li, G., and Li, H. (1995). Selective binding and removal of guests in a microporous metal-organic framework. Nature *378*, 703–706.

91. Takaishi, S., Hosoda, M., Kajiwara, T., Miyasaka, H., Yamashita, M., Nakanishi, Y., Kitagawa, Y., Yamaguchi, K., Kobayashi, A., and Kitagawa, H. (2009). Electroconductive porous coordination polymer Cu[Cu(pdt)$_2$] composed of donor and acceptor building units. Inorg. Chem. *48*, 9048–9050.

92. Herm, Z.R., Wiers, B.M., Mason, J.A., van Baten, J.M., Hudson, M.R., Zajdel, P., Brown, C.M., Masciocchi, N., Krishna, R., and Long, J.R. (2013). Separation of hexane isomers in a metal-organic framework with triangular channels. Science *340*, 960–964.

93. Aubrey, M.L., Wiers, B.M., Andrews, S.C., Sakurai, T., Reyes-Lillo, S.E., Hamed, S.M., Yu, C.J., Darago, L.E., Mason, J.A., Baeg, J.O., et al. (2018). Electron delocalization and charge mobility as a function of reduction in a metal-organic framework. Nat. Mater. *17*, 625–632.

94. Xie, L.S., Sun, L., Wan, R., Park, S.S., DeGayner, J.A., Hendon, C.H., and Dincă, M. (2018). Tunable mixed-valence doping toward record electrical conductivity in a three-dimensional metal-organic framework. J. Am. Chem. Soc. *140*, 7411–7414.

95. Gándara, F., Uribe-Romo, F.J., Britt, D.K., Furukawa, H., Lei, L., Cheng, R., Duan, X., O'Keeffe, M., and Yaghi, O.M. (2012). Porous, conductive metal-triazolates and their structural elucidation by the charge-flipping method. Chemistry *18*, 10595–10601.

96. Narayan, T.C., Miyakai, T., Seki, S., and Dincă, M. (2012). High charge mobility in a tetrathiafulvalene-based microporous metal-organic framework. J. Am. Chem. Soc. *134*, 12932–12935.

97. Goetz, K.P., Vermeulen, D., Payne, M.E., Kloc, C., McNeil, L.E., and Jurchescu, O.D. (2014). Charge-transfer complexes: new perspectives on an old class of compounds. J. Mater. Chem. C *2*, 3065–3076.

98. Talin, A.A., Centrone, A., Ford, A.C., Foster, M.E., Stavila, V., Haney, P., Kinney, R.A., Szalai, V., El Gabaly, F.E., Yoon, H.P., et al. (2014). Tunable electrical conductivity in metal-organic framework thin-film devices. Science *343*, 66–69.

99. Bhadra, B.N., Ahmed, I., Lee, H.J., and Jhung, S.H. (2022). Metal-organic frameworks bearing free carboxylic acids: preparation, modification, and applications. Coord. Chem. Rev. *450*, 214237.

100. Kökçam-Demir, Ü., Goldman, A., Esrafili, L., Gharib, M., Morsali, A., Weingart, O., and Janiak, C. (2020). Coordinatively unsaturated metal sites (open metal sites) in metal-organic frameworks: design and applications. Chem. Soc. Rev. *49*, 2751–2798.

101. Banerjee, M.D., Das, S., Yoon, M., Choi, H.J., Hyun, M.H., Park, S.M., Seo, G., and Kim, K. (2009). Postsynthetic modification switches an achiral framework to catalytically active homochiral metal-organic porous materials. J. Am. Chem. Soc. *131*, 7524–7525.

102. Wiers, B.M., Foo, M.L., Balsara, N.P., and Long, J.R. (2011). A solid lithium electrolyte via addition of lithium isopropoxide to a metal-organic framework with open metal sites. J. Am. Chem. Soc. *133*, 14522–14525.

103. Sarango-Ramírez, M.K., Park, J., Kim, J., Yoshida, Y., Lim, D.W., and Kitagawa, H. (2021). Void space versus surface functionalization for proton conduction in metal-organic frameworks. Angew. Chem. Int. Ed. Engl. *60*, 20173–20177.

104. Van Humbeck, J.F., Aubrey, M.L., Alsbaiee, A., Ameloot, R., Coates, G.W., Dichtel, W.R., and Long, J.R. (2015). Tetraarylborate polymer networks as single-ion conducting solid electrolytes. Chem. Sci. *6*, 5499–5505.

105. Aubrey, M.L., Ameloot, R., Wiers, B.M., and Long, J.R. (2014). Metal–organic frameworks as solid magnesium electrolytes. Energy Environ. Sci. *7*, 667.

106. Su, J., He, W., Li, X.-M., Sun, L., Wang, H.-Y., Lan, Y.-Q., Ding, M., and Zuo, J.-L. (2020). High electrical conductivity in a 2D MOF with intrinsic superprotonic conduction and interfacial pseudo-capacitance. Matter *2*, 711–722.

107. Das, K.S., Pal, B., Saha, S., Akhtar, S., De, A., Ray, P.P., and Mondal, R. (2020). Utilization of counter anions for charge transportation in the electrical device fabrication of Zn(II) metal-organic frameworks. Dalton Trans. *49*, 17005–17016.

108. Bi, S., Banda, H., Chen, M., Niu, L., Chen, M., Wu, T., Wang, J., Wang, R., Feng, J., Chen, T., et al. (2020). Molecular understanding of charge storage and charging dynamics in supercapacitors with MOF electrodes and

ionic liquid electrolytes. Nat. Mater. *19*, 552–558.

109. Zanca, F., Glasby, L.T., Chong, S., Chen, S., Kim, J., Fairen-Jimenez, D., Monserrat, B., and Moghadam, P.Z. (2021). Computational techniques for characterisation of electrically conductive MOFs: quantum calculations and machine learning approaches. J. Mater. Chem. C *9*, 13584–13599.

110. Hu, Z., Castano, I., Wang, S., Wang, Y., Peng, Y., Qian, Y., Chi, C., Wang, X., and Zhao, D. (2016). Modulator effects on the water-based synthesis of Zr/Hf metal–organic frameworks: quantitative relationship studies between modulator, synthetic condition, and performance. Cryst. Growth Des. *16*, 2295–2301.

111. Hausdorf, S., Baitalow, F., Seidel, J., and Mertens, F.O.R.L. (2007). Gaseous species as reaction tracers in the solvothermal synthesis of the zinc oxide terephthalate MOF-5. J. Phys. Chem. A *111*, 4259–4266.

112. Li, H.E., Eddaoudi, M., O'Keeffe, M., and Yaghi, O.M. (1999). Design and synthesis of an exceptionally stable and highly porous metal-organic framework. Nature *402*, 276–279.

113. Chen, T., Dou, J.H., Yang, L., Sun, C., Oppenheim, J.J., Li, J., and Dincă, M. (2022). Dimensionality modulates electrical conductivity in compositionally constant one-, two-, and three-dimensional frameworks. J. Am. Chem. Soc. *144*, 5583–5593.

114. Hausdorf, S.W., Wagler, J., Mossig, R., and Mertens, F.O.R.L. (2008). Proton and water activity-controlled structure formation in zinc carboxylate-based metal organic frameworks. J. Phys. Chem. A *112*, 7567–7576.

115. Goesten, M., Stavitski, E., Pidko, E.A., Gücüyener, C., Boshuizen, B., Ehrlich, S.N., Hensen, E.J., Kapteijn, F., and Gascon, J. (2013). The molecular pathway to ZIF-7 microrods revealed by in situ time-resolved small- and wide-angle X-ray scattering, quick-scanning extended X-ray absorption spectroscopy, and DFT calculations. Chemistry *19*, 7809–7816.

116. Park, J., Hinckley, A.C., Huang, Z., Feng, D., Yakovenko, A.A., Lee, M., Chen, S., Zou, X., and Bao, Z. (2018). Synthetic routes for a 2D semiconductive copper hexahydroxybenzene metal-organic framework. J. Am. Chem. Soc. *140*, 14533–14537.

117. Schaate, A., Roy, P., Godt, A., Lippke, J., Waltz, F., Wiebcke, M., and Behrens, P. (2011). Modulated synthesis of Zr-based metal-organic frameworks: from Nano to single crystals. Chemistry *17*, 6643–6651.

118. Ma, T., Kapustin, E.A., Yin, S.X., Liang, L., Zhou, Z., Niu, J., Li, L.H., Wang, Y., Su, J., Li, J., et al. (2018). Single-crystal x-ray diffraction structures of covalent organic frameworks. Science *361*, 48–52.

119. Marshall, R.J., Hobday, C.L., Murphie, C.F., Griffin, S.L., Morrison, C.A., Moggach, S.A., and Forgan, R.S. (2016). Amino acids as highly efficient modulators for single crystals of zirconium and hafnium metal–organic frameworks. J. Mater. Chem. A *4*, 6955–6963.

120. Cheetham, A.K., Kieslich, G., and Yeung, H.H. (2018). Thermodynamic and kinetic effects in the crystallization of metal-organic frameworks. Acc. Chem. Res. *51*, 659–667.

121. Borysiewicz, M.A., Dou, J.H., Stassen, I., and Dincă, M. (2021). Why conductivity is not always king - physical properties governing the capacitance of 2D metal-organic framework-based EDLC supercapacitor electrodes: a $Ni_3(HITP)_2$ case study. Faraday Discuss. *231*, 298–304.

122. Moosavi, S.M., Chidambaram, A., Talirz, L., Haranczyk, M., Stylianou, K.C., and Smit, B. (2019). Capturing chemical intuition in synthesis of metal-organic frameworks. Nat. Commun. *10*, 539.

123. Springer, S.E., Mihaly, J.J., Amirmokhtari, N., Crom, A.B., Zeller, M., Feldblyum, J.I., and Genna, D.T. (2019). Framework isomerism in a series of btb-containing in-derived metal–organic frameworks. Cryst. Growth Des. *19*, 3124–3129.

124. Shearer, G.C., Chavan, S., Ethiraj, J., Vitillo, J.G., Svelle, S., Olsbye, U., Lamberti, C., Bordiga, S., and Lillerud, K.P. (2014). Tuned to perfection: ironing out the defects in metal–organic framework UiO-66. Chem. Mater. *26*, 4068–4071.

125. Katz, M.J., Brown, Z.J., Colón, Y.J., Siu, P.W., Scheidt, K.A., Snurr, R.Q., Hupp, J.T., and Farha, O.K. (2013). A facile synthesis of UiO-66, UiO-67 and their derivatives. Chem. Commun. (Camb) *49*, 9449–9451.

126. Ma, J., Kalenak, A.P., Wong-Foy, A.G., and Matzger, A.J. (2017). Rapid guest exchange and ultra-low surface tension solvents optimize metal-organic framework activation. Angew. Chem. Int. Ed. Engl. *56*, 14618–14621.

127. Mondloch, J.E., Karagiaridi, O., Farha, O.K., and Hupp, J.T. (2013). Activation of metal–organic framework materials. CrystEngComm *15*, 9258.

128. Nelson, A.P.F., Farha, O.K., Mulfort, K.L., and Hupp, J.T. (2009). Supercritical processing as a route to high internal surface areas and permanent microporosity in metal-organic framework materials. J. Am. Chem. Soc. *131*, 458–460.

129. Guo, H., Zhu, Y., Wang, S., Su, S., Zhou, L., and Zhang, H. (2012). Combining coordination modulation with acid–base adjustment for the control over size of metal–organic frameworks. Chem. Mater. *24*, 444–450.

130. Kyerematen, N.A., Brousse, T., and Pech, D. (2017). Microsupercapacitors as miniaturized energy-storage components for on-chip electronics. Nat. Nanotechnol. *12*, 7–15.

131. Martí-Rujas, J. (2020). Structural elucidation of microcrystalline MOFs from powder X-ray diffraction. Dalton Trans. *49*, 13897–13916.

132. Han, J., He, X., Liu, J., Ming, R., Lin, M., Li, H., Zhou, X., and Deng, H. (2022). Determining factors in the growth of MOF single crystals unveiled by in situ interface imaging. Chem *8*, 1637–1657.

133. Dou, J.H., Arguilla, M.Q., Luo, Y., Li, J., Zhang, W., Sun, L., Mancuso, J.L., Yang, L., Chen, T., Parent, L.R., et al. (2021). Atomically precise single-crystal structures of electrically conducting 2D metal-organic frameworks. Nat. Mater. *20*, 222–228.

134. Wiktor, C., Meledina, M., Turner, S., Lebedev, O.I., and Fischer, R.A. (2017). Transmission electron microscopy on metal–organic frameworks – a review. J. Mater. Chem. A *5*, 14969–14989.

135. Kondo, A.N., Noguchi, H., Carlucci, L., Proserpio, D.M., Ciani, G., Kajiro, H., Ohba, T., Kanoh, H., and Kaneko, K. (2007). Double-step gas sorption of a two-dimensional metal-organic framework. J. Am. Chem. Soc. *129*, 12362–12363.

136. Pütz, A.M., Terban, M.W., Bette, S., Haase, F., Dinnebier, R.E., and Lotsch, B.V. (2020). Total scattering reveals the hidden stacking disorder in a 2D covalent organic framework. Chem. Sci. *11*, 12647–12654.

137. Bennett, T.D., Goodwin, A.L., Dove, M.T., Keen, D.A., Tucker, M.G., Barney, E.R., Soper, A.K., Bithell, E.G., Tan, J.C., and Cheetham, A.K. (2010). Structure and properties of an amorphous metal-organic framework. Phys. Rev. Lett. *104*, 115503.

138. Fonseca, J., Gong, T., Jiao, L., and Jiang, H.-L. (2021). Metal–organic frameworks (MOFs) beyond crystallinity: amorphous MOFs, MOF liquids and MOF glasses. J. Mater. Chem. A *9*, 10562–10611.

139. Shearer, G.C., Chavan, S., Bordiga, S., Svelle, S., Olsbye, U., and Lillerud, K.P. (2016). Defect engineering: tuning the porosity and composition of the metal–organic framework UiO-66 via modulated synthesis. Chem. Mater. *28*, 3749–3761.

140. Feldblyum, J.I., Liu, M., Gidley, D.W., and Matzger, A.J. (2011). Reconciling the discrepancies between crystallographic porosity and guest access as exemplified by Zn-HKUST-1. J. Am. Chem. Soc. *133*, 18257–18263.

141. Banda, H., Dou, J.H., Chen, T., Libretto, N.J., Chaudhary, M., Bernard, G.M., Miller, J.T., Michaelis, V.K., and Dincă, M. (2021). High-capacitance pseudocapacitors from Li^+ ion intercalation in nonporous, electrically conductive 2D coordination polymers. J. Am. Chem. Soc. *143*, 2285–2292.

142. Brunauer, S., Emmett, P.H., and Teller, E. (1938). Adsorption of gases in multimolecular layers. J. Am. Chem. Soc. *60*, 309–319.

143. Gregg, S.J., and Sing, K.S.W. (2020). Adsorption, Surface Area and Porosity (Second Edition, Academic Press).

144. Soldatov, M.A., Martini, A., Bugaev, A.L., Pankin, I., Medvedev, P.V., Guda, A.A., Aboraia, A.M., Podkovyrina, Y.S., Budnyk, A.P., Soldatov, A.A., and Lamberti, C. (2018). The insights from X-ray absorption spectroscopy into the local atomic structure and chemical bonding of metal–organic frameworks. Polyhedron *155*, 232–253.

145. Dou, J.H., Sun, L., Ge, Y., Li, W., Hendon, C.H., Li, J., Gul, S., Yano, J., Stach, E.A., and Dincă, M. (2017). Signature of metallic behavior in the metal-organic frameworks M_3(hexaiminobenzene)$_2$ (M = Ni, Cu). J. Am. Chem. Soc. *139*, 13608–13611.

146. Sheberla, D., Sun, L., Blood-Forsythe, M.A., Er, S., Wade, C.R., Brozek, C.K., Aspuru-Guzik, A., and Dincă, M. (2014). High electrical conductivity in Ni_3(2,3,6,7,10,11-hexaiminotriphenylene)$_2$, a semiconducting

metal-organic graphene analogue. J. Am. Chem. Soc. *136*, 8859–8862.

147. Sun, L., Hendon, C.H., Park, S.S., Tulchinsky, Y., Wan, R., Wang, F., Walsh, A., and Dincă, M. (2017). Is iron unique in promoting electrical conductivity in MOFs? Chem. Sci. *8*, 4450–4457.

148. Dean, J.R. (2007). Practical Inductively Coupled Plasma Spectroscopy (Wiley).

149. Chu, J., Ke, F.S., Wang, Y., Feng, X., Chen, W., Ai, X., Yang, H., and Cao, Y. (2020). Facile and reversible digestion and regeneration of zirconium-based metal-organic frameworks. Commun. Chem. *3*, 5.

150. Yang, F., Feng, X., Liu, Y.-S., Kao, L.C., Glans, P.-A., Yang, W., and Guo, J. (2021). In situ/operando (soft) X-ray spectroscopy study of beyond lithium-ion batteries. Energy Environ. Mater. *4*, 139–157.

151. Lin, F., Liu, Y., Yu, X., Cheng, L., Singer, A., Shpyrko, O.G., Xin, H.L., Tamura, N., Tian, C., Weng, T.C., et al. (2017). Synchrotron X-ray analytical techniques for studying materials electrochemistry in rechargeable batteries. Chem. Rev. *117*, 13123–13186.

152. Balasubramanian, M.S., Sun, X., Yang, X.Q., and McBreen, J. (2001). In situ X-ray diffraction and X-ray absorption studies of high-rate lithium-ion batteries. J. Power Sources *92*, 1–8.

153. Hua, W., Wang, S., Knapp, M., Leake, S.J., Senyshyn, A., Richter, C., Yavuz, M., Binder, J.R., Grey, C.P., Ehrenberg, H., et al. (2019). Structural insights into the formation and voltage degradation of lithium- and manganese-rich layered oxides. Nat. Commun. *10*, 5365.

154. Li, C., Hu, X., Lou, X., Zhang, L., Wang, Y., Amoureux, J.-P., Shen, M., Chen, Q., and Hu, B. (2016). The organic-moiety-dominated Li^+ intercalation/deintercalation mechanism of a cobalt-based metal–organic framework. J. Mater. Chem. A *4*, 16245–16251.

155. Bak, S.-M., Shadike, Z., Lin, R., Yu, X., and Yang, X.-Q. (2018). In situ/operando synchrotron-based X-ray techniques for lithium-ion battery research. NPG Asia Mater. *10*, 563–580.

156. Qiao, R., Xia, Y., Feng, X., Macdougall, J., Pepper, J., Armitage, K., Borsos, J., Knauss, K.G., Lee, N., Allézy, A., et al. (2018). Soft x-ray spectroscopy of high pressure liquid. Rev. Sci. Instrum. *89*, 013114.

157. Park, J., Lee, M., Feng, D., Huang, Z., Hinckley, A.C., Yakovenko, A., Zou, X., Cui, Y., and Bao, Z. (2018). Stabilization of hexaaminobenzene in a 2D conductive metal–organic framework for high power sodium storage. J. Am. Chem. Soc. *140*, 10315–10323.

158. Wi, S., Shutthanandan, V., Sivakumar, B.M., Thevuthasan, S., Prabhakaran, V., Roy, S., Karakoti, A., and Murugesan, V. (2022). In situ X-ray photoelectron spectroscopy analysis of electrochemical interfaces in battery: recent advances and remaining challenges. J. Vac. Sci. Technol. A *40*, 010808.

159. Li, C.-Y., Yu, Y., Wang, C., Zhang, Y., Zheng, S.-Y., Li, J.-F., Maglia, F., Jung, R., Tian, Z.-Q., and Shao-Horn, Y. (2020). Surface changes of $LiNi_xMn_yCo_{1-x-y}O_2$ in Li-ion batteries using in situ surface-enhanced Raman spectroscopy. J. Phys. Chem. C *124*, 4024–4031.

160. Louarn, G.L., Lapkowski, M., Quillard, S., Pron, A., Buisson, J.P., and Lefrant, S. (1996). Vibrational properties of polyanilines isotope effects. J. Phys. Chem. *100*, 6998–7006.

161. Bitenc, J., Vizintin, A., Grdadolnik, J., and Dominko, R. (2019). Tracking electrochemical reactions inside organic electrodes by operando IR spectroscopy. Energy Storage Mater. *21*, 347–353.

162. Zhao, Q., Huang, W., Luo, Z., Liu, L., Lu, Y., Li, Y., Li, L., Hu, J., Ma, H., and Chen, J. (2018). High-capacity aqueous zinc batteries using sustainable quinone electrodes. Sci. Adv. *4*, eaao1761.

163. Samajdar, R.N., Brown, S.A., Kairy, S.K., Robertson, S.D., and Wain, A.J. (2022). Methodologies for operando ATR-IR spectroscopy of magnesium battery electrolytes. Anal. Chem. *94*, 14985–14993.

164. Liu, J., Xie, D., Xu, X., Jiang, L., Si, R., Shi, W., and Cheng, P. (2021). Reversible formation of coordination bonds in Sn-based metal-organic frameworks for high-performance lithium storage. Nat. Commun. *12*, 3131.

165. Levi, M.D., Daikhin, L., Aurbach, D., and Presser, V. (2016). Quartz crystal microbalance with dissipation monitoring (EQCM-D) for in-situ studies of electrodes for supercapacitors and batteries: a mini-review. Electrochem. Commun. *67*, 16–21.

166. Levi, M.D., Lukatskaya, M.R., Sigalov, S., Beidaghi, M., Shpigel, N., Daikhin, L., Aurbach, D., Barsoum, M.W., and Gogotsi, Y. (2015). Solving the capacitive paradox of 2D MXene using electrochemical quartz-crystal admittance and in situ electronic conductance measurements. Adv. Energy Mater. *5*, 1400815.

167. He, T., Kong, X.J., and Li, J.R. (2021). Chemically stable metal-organic frameworks: rational construction and application expansion. Acc. Chem. Res. *54*, 3083–3094.

168. Zheng, W., Liu, M., and Lee, L.Y.S. (2019). Electrochemical instability of metal–organic frameworks: in situ spectroelectrochemical investigation of the real active sites. ACS Catal. *10*, 81–92.

169. Wang, L., Han, Y., Feng, X., Zhou, J., Qi, P., and Wang, B. (2016). Metal–organic frameworks for energy storage: batteries and supercapacitors. Coord. Chem. Rev. *307*, 361–381.

170. Zhao, R., Liang, Z., Zou, R., and Xu, Q. (2018). Metal-organic frameworks for batteries. Joule *2*, 2235–2259.

171. Lee, M., Hong, J., Lopez, J., Sun, Y., Feng, D., Lim, K., Chueh, W.C., Toney, M.F., Cui, Y., and Bao, Z. (2017). High-performance sodium–organic battery by realizing four-sodium storage in disodium rhodizonate. Nat. Energy *2*, 861–868.

172. Jurng, S., Heiskanen, S.K., Chandrasiri, K.W.D.K., Abeywardana, M.Y., and Lucht, B.L. (2019). Minimized metal dissolution from high-energy nickel cobalt manganese oxide cathodes with Al_2O_3 coating and its effects on electrolyte decomposition on graphite anodes. J. Electrochem. Soc. *166*, A2721–A2726.

173. Bunzen, H. (2021). Chemical stability of metal-organic frameworks for applications in drug delivery. ChemNanoMat *7*, 998–1007.

174. Wang, H., Rus, E., Sakuraba, T., Kikuchi, J., Kiya, Y., and Abruña, H.D. (2014). CO_2 and O_2 evolution at high voltage cathode materials of Li-ion batteries: a differential electrochemical mass spectrometry study. Anal. Chem. *86*, 6197–6201.

175. Imhof, R., and Novák, P. (1999). Oxidative electrolyte solvent degradation in lithium-ion batteries: an in situ differential electrochemical mass spectrometry investigation. J. Electrochem. Soc. *146*, 1702–1706.

176. He, Y.C., Cubuk, E.D., Allendorf, M.D., and Reed, E.J. (2018). Metallic metal−organic frameworks predicted by the combination of machine learning methods and ab initio calculations. J. Phys. Chem. Lett. *9*, 4562–4569.

177. Largeot, C., Portet, C., Chmiola, J., Taberna, P.-L., Gogotsi, Y., and Simon, P. (2008). Relation between the ion size and pore size for an electric double-layer capacitor. J. Am. Chem. Soc. *130*, 2730–2731.